

REMARKS

Summary of Telephone Interview

Applicants wish to kindly thank the Examiner for offering her time and helpful comments during a telephone discussion with Applicants' representative on December 18, 2008. During this conversation, the Examiner indicated that since the subject matter of the amended claims was part of the originally elected group I, it would be acceptable to amend the claims as shown above in an Amendment After Final Rejection. Specifically, the Examiner indicated that the scope of the amended claims would have been included in her original search, and thus any applicable art would likely have been cited in the first Office Action on the merits.

Again, Applicants kindly thank the Examiner for her helpful comments.

Claim Amendments

Applicants have amended claim 1 to recite compounds of formula (1), wherein R¹ is a carboxyl group, and X is CH₂, CHF, CF₂, or CHOH. As mentioned above, the scope of the amended claims falls within the scope of elected Group I.

New claim 10 has been added to the application, and is directed to the particular compound recited on page 11, lines 2-3 of Applicants' specification.

Accordingly, no new matter has been added to the application by these amendments.

Consideration After Final Rejection

Although this amendment is presented after final rejection, the Examiner is respectfully requested to enter the amendments and consider the remarks, as they place the application in condition for allowance.

Patentability Arguments

The patentability of the present invention over the disclosures of the references relied upon by the Examiner in rejecting the claims will be apparent upon consideration of the following remarks.

Rejection Under 35 U.S.C. § 103(a)

The rejection of claims 1 and 6 under 35 U.S.C. § 103(a) as being unpatentable over Haffner et al. (WO 2003/002553) in view of Villhauer (WO 98/19998) has been rendered moot by the above-discussed claim amendments.

Specifically, the amended claims no longer encompass a compound wherein R¹ is methyl. Accordingly, the above rejection is no longer tenable, and Applicants respectfully request its withdrawal.

Discussion Regarding US 2004/0072892

Additionally, in order to expedite allowance of this application, Applicants submit the following remarks in support of the patentability of the presently claimed invention over the disclosure of US 2004/0072892, which was cited in the Information Disclosure Statement filed February 20, 2008. Favorable consideration is respectfully requested in view of these remarks.

The amended claims are directed to a bicyclo derivative represented by recited formula (1), wherein R¹ is carboxyl.

Applicants acknowledge that US 2004/0072892 (US '892) teaches a genus which encompasses Applicants' claimed species. However, MPEP 2144.08(II) indicates that "[t]he fact that a claimed species or subgenus is encompassed by a prior art genus is not sufficient by itself to establish a *prima facie* case of obviousness. *In re Baird*, 16 F.3d 380, 382 (Fed. Cir. 1994)."

US '892 fails to expressly disclose Applicants' particularly claimed compound. Specifically, there is no example in US '892 wherein R¹ is a carboxylic acid moiety. Accordingly, US '892 fails to anticipate the claims of the present application. Thus, the following remarks relate to obviousness of a species when the cited prior art teaches the genus. This situation is discussed in detail in MPEP 2144.08.

One of ordinary skill in the art would not have been motivated
to select the claimed species of subgenus

MPEP 2144.08(II)(A)(4) sets forth factors for consideration in determining whether one of ordinary skill in the art would have been motivated to select the claimed species or subgenus from the disclosed prior art genus.

Initially, the size of the genus is to be considered. The Court of Customs and Patent Appeals (CCPA) found that a prior art genus containing only 20 compounds and a limited number of variations in the generic chemical formula anticipated a claimed species within the genus, because one skilled in the art would envisage each member of the genus. *See In re Petering*, 30 F.2d 676, 681 (CCPA 1962). The *Petering* court stated, “. . . we wish to point out that it is not the mere number of compounds here but, rather, the total circumstances involved, including such factors as the limited number of variations for R, only two alternatives for Y and Z, no alternatives for the other ring positions, and a large unchanging parent structural nucleus.” Additionally, the CCPA also found that the rejection of a claimed compound in light of a prior art genus based on *Petering* is not appropriate where the prior art does not disclose a small recognizable class of compounds with common properties. *In re Ruschig*, 343 F.2d 965, 974 (CCPA 1965).

In the present situation, the general Formula (1) of US ‘892 includes 7 variables, and each variable (except X) has *many* variations. Accordingly, it is clear that this situation does not fall within the meaning of *Petering*, as discussed above. Specifically, it cannot be said that US ‘892 “described each of the various permutations here involved as fully as if he had drawn each structural formula or written each name,” as the court discussed in the *Petering* case.

Therefore, one of ordinary skill in the art would not have been motivated to select Applicants’ claimed compound from the disclosed genus of US ‘892.

Structural differences between compounds of US ‘892
and Applicants’ claimed compounds

MPEP 2144.08(II)(A)(2) states that the Examiner should compare the disclosed prior art genus and that of any expressly described species or subgenus within the genus to the claimed

species or subgenus to determine the differences. Specifically, the closest disclosed species or subgenus in the reference should be identified and compared to that claimed.

Applicants consider that the compound of Example 33 of US '892 is the most structurally similar to the compounds of Applicants' claims, specifically to the compound of Applicants' new claim 10, i.e., the compound of Applicants' Example 1. However, the compound of Example 33 of US '892 differs from the compound of Applicants' Example 1 in the following ways: Example 33 has a different ring structure than Example 1; and Example 33 does not have a carboxyl group, as in Example 1.

Accordingly, several variables must be selected and modified to achieve Applicants' claimed compound from the compound of Example 33 of US '892.

The Examiner is reminded that the question under 35 U.S.C. 103(a) is not whether the differences between the claimed invention and the prior art would have been obvious, but whether the claimed invention *as a whole* would have been obvious. *See Stratoflex, Inc. v. Aeroquip Corp.*, 713 F.2d 1530, 1537 (Fed. Cir. 1983).

Unexpected and superior results of Applicants' claimed compounds

The following discussion refers to the compound of Applicants' Example 1, which, as stated above, is the compound recited in Applicants' new claim 10. Accordingly, this compound clearly falls within the scope of Applicants' independent claim 1.

The compound of Applicants' Example 1 has unexpected results when compared to the compounds of US '892.

DPP4 inhibitors, such as the compound of Applicants' Example 1, exert their pharmacologic effect by inhibiting the activity of DPP4 in the blood, as DPP4 is present in the blood, and not in the cell.

It is considered that side effects which had been previously attributed to DPP4 inhibition (such as toxicity and effects on immune function) are actually caused by inhibition of DPP9 activity. (Please see the reference document, enclosed as Attachment A). DPP9 exists in the cells. (Please see the reference document, enclosed as Attachment B.) Accordingly, any

compound that cannot pass through the cell membrane (and into the cell) cannot inhibit the activity of DPP9, thus avoiding the negative side effects.

Applicants have discovered compounds (i.e., the Example 1 Compound), which are selective DPP4 inhibitors. In other words, the compound of Applicants' Example 1 is present in the blood, and thus inhibits DPP4, which is also present in the blood. However, the compound of Applicants' Example 1 has very low cell membrane permeability, and thus does not permeate through the cell membrane, into the cell, to inhibit DPP9. This property (selective DPP4 inhibition) clearly distinguishes the compound of Applicants' Example 1 (and new claim 10) from the compounds disclosed in US '892.

Applicants have conducted several experiments using the compound of Example 1 to determine the DPP9 inhibitory activity in the cases of "Cell-Free" and "Cell-Base". The results are shown below in Table 1.

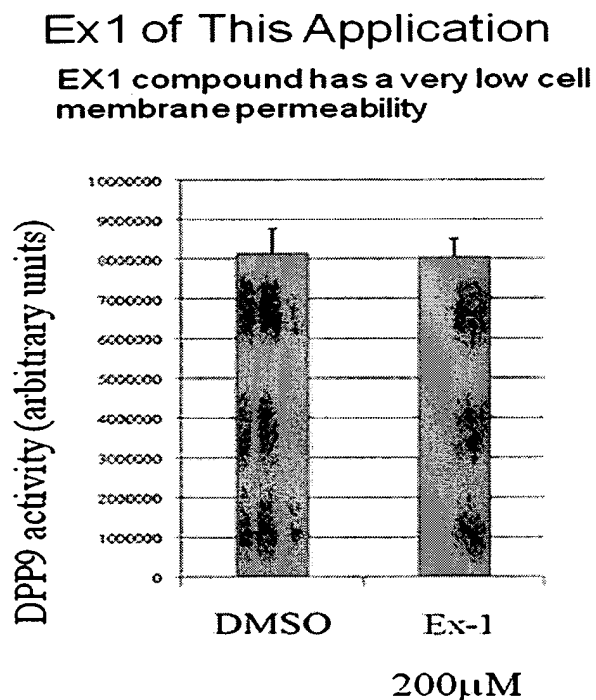
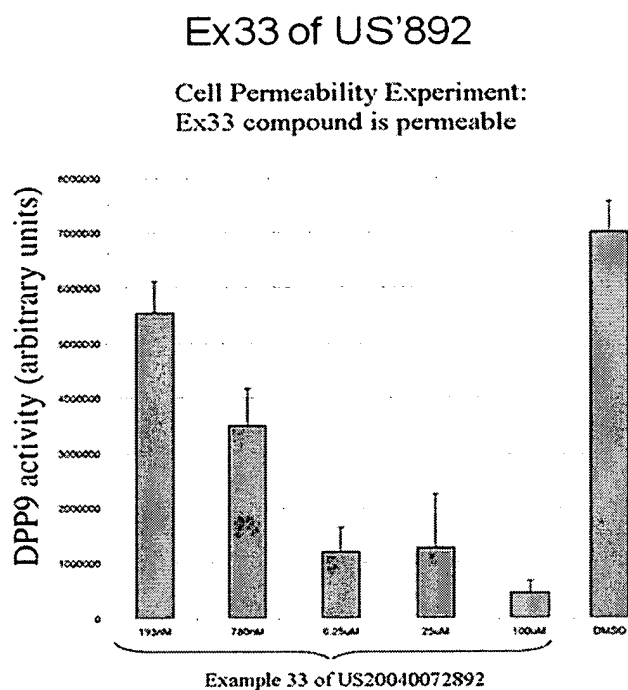
Table 1

Conc. Of Applicants' Example 1 Compound (μ M)	Relative DPP9 activity (%) (Cell-Free)	Relative DPP9 activity (%) (Cell-Based)
0	100	100
0.32	92.9	(Not Tested)
1.6	56.5	(Not Tested)
8	18.5	(Not Tested)
20	0	117

As shown in Table 1 above, the compound of Applicants' Example 1 shows DPP9 inhibitory activity in the case of Cell-Free, but does not show such DPP9 inhibitory activity in the case of Cell-Base. This is due to the lack of cell membrane permeability of the compounds of Applicants' claims.

On the contrary, the compounds disclosed in the examples of US '892 have cell membrane permeability, and accordingly have DPP9 inhibitory activity in the cell.

As mentioned previously, Applicants consider the compound of Example 33 of US '892 to have the most similar structure to the compounds of Applicants' claims. Applicants have determined the DPP9 inhibitory activity in cell of Example 33 of US '892, and compared it to the DPP inhibitory activity of the compound of Applicants' Example 1. Please see the Figures below, which show DPP9 activity of Example 33 of US '892 and the compound of Applicants' Example 1.



It is clear from the above Figures that increased presence of the compound of Example 33 of US '892 inhibits DPP9 activity. On the contrary, the presence of the compound of Applicants' Example 1 does not inhibit DPP9 activity. Accordingly, it is clear that Applicants' claimed compounds have unexpected and superior results when compared to the compounds of US '892. Specifically, Applicants' claimed compounds are selective DPP4 inhibitors, resulting in fewer side effects, due to the lack of DPP9 inhibition.

Accordingly, although Applicants' claimed species falls within the genus of US '892, it is clear that the reference does not anticipate or render obvious Applicants' recited species.

Conclusion

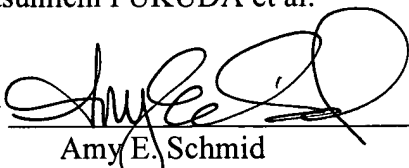
Therefore, in view of the foregoing amendments and remarks, it is submitted that the ground of rejection set forth by the Examiner has been overcome, and that the application is in condition for allowance. Such allowance is solicited.

Additionally, in view of the foregoing remarks, it is submitted that Applicants' claims are clearly patentable over the disclosure of US '892. Applicants respectfully assert that the present application is in condition for allowance. Such allowance is respectfully solicited.

If, after reviewing this Amendment, the Examiner feels there are any issues remaining which must be resolved before the application can be passed to issue, the Examiner is respectfully requested to contact the undersigned by telephone in order to resolve such issues.

Respectfully submitted,

Yasumichi FUKUDA et al.

By 

Amy E. Schmid
Registration No. 55,965
Attorney for Applicants

AES/emj
Washington, D.C. 20006-1021
Telephone (202) 721-8200
Facsimile (202) 721-8250
December 19, 2008

Original Article

Dipeptidyl Peptidase IV Inhibition for the Treatment of Type 2 Diabetes

Potential Importance of Selectivity Over Dipeptidyl Peptidases 8 and 9

George R. Lankas,¹ Barbara Leiting,² Ranabir Sinha Roy,² George J. Eiermann,³ Maria G. Beconi,⁴ Tesfaye Biftu,⁵ Chi-Chung Chan,⁶ Scott Edmondson,⁵ William P. Feeney,⁷ Huaibing He,⁵ Dawn E. Ippolito,³ Dooseop Kim,⁵ Kathryn A. Lyons,⁵ Hyun O. Ok,⁵ Reshma A. Patel,² Aleksandr N. Petrov,³ Kelly Ann Pryor,² Xiaoxia Qian,⁵ Leah Reigle,⁵ Andrea Woods,⁸ Joseph K. Wu,² Dennis Zaller,⁸ Xiaoping Zhang,² Lan Zhu,² Ann E. Weber,⁵ and Nancy A. Thornberry²

Dipeptidyl peptidase (DPP)-IV inhibitors are a new approach to the treatment of type 2 diabetes. DPP-IV is a member of a family of serine peptidases that includes quiescent cell proline dipeptidase (QPP), DPP8, and DPP9; DPP-IV is a key regulator of incretin hormones, but the functions of other family members are unknown. To determine the importance of selective DPP-IV inhibition for the treatment of diabetes, we tested selective inhibitors of DPP-IV, DPP8/DPP9, or QPP in 2-week rat toxicity studies and in acute dog tolerability studies. In rats, the DPP8/9 inhibitor produced alopecia, thrombocytopenia, reticulocytopenia, enlarged spleen, multiorgan histopathological changes, and mortality. In dogs, the DPP8/9 inhibitor produced gastrointestinal toxicity. The QPP inhibitor produced reticulocytopenia in rats only, and no toxicities were noted in either species for the selective DPP-IV inhibitor. The DPP8/9 inhibitor was also shown to attenuate T-cell activation in human in vitro models; a selective DPP-IV inhibitor was inactive in these assays. Moreover, we found DPP-IV inhibitors that were previously reported to be active in models of immune function to be more potent inhibitors of DPP8/9. These results suggest that assessment of selectivity of potential clinical candidates may be

important to an optimal safety profile for this new class of antihyperglycemic agents. *Diabetes* 54:2988–2994, 2005

Therapies that increase the circulating concentrations of insulin have proven beneficial in the treatment of type 2 diabetes. Dipeptidyl peptidase (DPP)-IV inhibitors are a promising new approach to type 2 diabetes that function, at least in part, as indirect stimulators of insulin secretion (1). Clinical proof of concept for the efficacy of DPP-IV inhibitors has been provided by LAF237 (2,3). Additional proof of concept has been obtained in studies with DPP-IV-deficient mice, which are healthy, fertile, and have improved metabolic function (4,5).

The efficacy of DPP-IV inhibitors is mediated primarily via stabilization of the incretin hormones glucagon-like peptide 1 (GLP-1) and glucose-dependent insulintropic polypeptide, which have clearly established roles in glucose-dependent insulin secretion (6). Subchronic (6 weeks) continuous infusion of GLP-1 resulted in profound and significant decreases in fasting plasma glucose and HbA_{1c} (1.3%) (7). GLP-1 is rapidly hydrolyzed ($t_{1/2} = \sim 1$ min) in vivo to produce an inactive product, GLP-1[9–36] amide (8), and several lines of evidence indicate that DPP-IV, a proline-specific serine dipeptidyl aminopeptidase, is primarily responsible for this inactivation (9,10).

DPP-IV is the founding member of a family of DPP-IV activity and/or structure homologue (DASH) proteins, enzymes that are unified by their common postproline cleaving serine dipeptidyl peptidase mechanism (11). In addition to DPP-IV, family members include quiescent cell proline dipeptidase (QPP) (aka DPP7) (12), DPP8 (13), DPP9 (14), fibroblast activation protein (15), attractin (16), and DPP-IV- β (17). Except for DPP-IV, the functions of these enzymes are unknown. Nonetheless, based on their preference for cleavage after H₂N-X-Pro in vitro, they are likely to be involved in at least some of the increasing number of biological processes that appear to be regulated by proline-specific NH₂-terminal processing (18). Thus,

From the ¹Department of Safety Assessment, Merck Research Laboratories, West Point, Pennsylvania; the ²Department of Metabolic Disorders, Merck Research Laboratories, Rahway, New Jersey; the ³Department of Pharmacology, Merck Research Laboratories, Rahway, New Jersey; the ⁴Department of Drug Metabolism, Merck Research Laboratories, Rahway, New Jersey; the ⁵Department of Medicinal Chemistry, Merck Research Laboratories, Rahway, New Jersey; the ⁶Merck Frosst Centre for Therapeutic Research, Pointe Claire, Dorval, Quebec, Canada; the ⁷Department of Laboratory Animal Resources, Merck Research Laboratories, Rahway, New Jersey; and the ⁸Department of Immunology, Merck Research Laboratories, Rahway, New Jersey.

Address correspondence and reprint requests to Nancy A. Thornberry, Merck Research Laboratories, R50G-2A-201, PO Box 2000, E. Lincoln Avenue, Rahway, New Jersey. E-mail: nancy_thornberry@merck.com.

Received for publication 3 March 2005 and accepted in revised form 20 July 2005.

M.G.B. is currently affiliated with GlaxoSmithKline. AMC, aminomethylcoumarin; DASH, DPP-IV activity and/or structure homologues; DPP, dipeptidyl peptidase; GLP-1, glucagon-like peptide 1; IL, interleukin; QPP, quiescent cell proline dipeptidase.

© 2005 by the American Diabetes Association.

The costs of publication of this article were defrayed in part by the payment of page charges. This article must therefore be hereby marked "advertisement" in accordance with 18 U.S.C. Section 1734 solely to indicate this fact.

given the unknown consequences of inhibiting one or more of these family members, a potentially important consideration in the selection of DPP-IV inhibitors for clinical development is the degree of selectivity over other DASH family proteins required for an optimal safety profile.

DPP-IV is identical to CD26, a marker for activated T-cells (19). There have been several studies with Lys [Z(NO₂)] pyrrolidide and related compounds aimed at investigating the potential role of enzyme activity in immune function (20). These compounds have been shown to have several effects on immune cells, including inhibition of proliferation, cytokine production, and induction of transforming growth factor- β secretion. However, the finding that there are several DPP-IV homologs has prompted reexamination of these results, as the selectivity of these compounds has not been reported.

Herein, we describe the results of studies with broad-specificity DASH inhibitors and highly selective inhibitors of DPP-IV, QPP, and DPP8/9 in *in vivo* models for the assessment of preclinical safety and tolerability and in *in vitro* models of T-cell activation.

RESEARCH DESIGN AND METHODS

Compounds. The *threo*-2*S*,3*S*-isoleucyl thiazolidine fumarate (2:1) (compound 1) was provided by the Department of Process Research, Merck Research Laboratories (Rahway, NJ). The *allo*-2*S*,3*R*-isoleucyl thiazolidine fumarate (2:1) (compound 2) was purchased from Heumann Pharma (Nuernberg, Germany). The (2*R*)-4-oxo-4-[3-(trifluoromethyl)-5,6-dihydro[1,2,4]triazolo [4,3-*a*]pyrazin-7(8*H*)-yl]-1-(2,5-difluorophenyl)butan-2-amine fumarate and hydrochloride salts (compound 3), (2*S*,3*R*)-2-(2-amino-3-methyl-1-oxopentan-1-yl)-1,3-dihydro-2*H*-isoinsole hydrochloride (compound 4), 1-[(2*S*)-2-amino-2-[(3*R*)-1-(4-iodophenyl)sulfonyl]pyrrolidin-3-yl]-1-oxoethylthiazolidine (compound 5), (2*S*)-2-[4-[[[(2*S*)-1-[(3*R*)-3-amino-4-(2,5-difluorophenyl)-1-oxobutyl]-2-pyrrolidinyl]carbonyl]amino]methyl]phenoxy]-3-methylbutanoic acid, trifluoroacetate (compound 6), [(2*R*)-1-*N*-valylpyrrolidin-2-yl]boronic acid, trifluoroacetate (compound 7), 4-nitrobenzyl [(5*S*)-5-amino-6-oxo-6-(1-pyrrolidinyl)hexyl]carbamate (compound 8), 4-nitrobenzyl [(5*S*)-5-amino-6-oxo-6-(1,3-thiazolidin-3-yl)hexyl]carbamate (compound 9), and 4-nitrobenzyl [(5*S*)-5-amino-6-oxo-6-(1-piperidinyl)hexyl]carbamate (compound 10) were provided by the Department of Medicinal Chemistry, Merck Research Laboratories (Rahway, NJ).

Pharmacokinetics of selective inhibitors. The pharmacokinetics of compounds 1 and 2 in rats and dogs were previously reported (21). Similar study protocols and methods of analyses were used to evaluate the pharmacokinetics of compounds 3, 4, and 5.

In vitro assays

DPP-IV. To measure the activity of DPP-IV, a continuous fluorometric assay was employed using Gly-Pro-AMC, which is cleaved by the enzyme to release the fluorescent aminomethylcoumarin (AMC). A typical reaction contained 50 pmol/l enzyme, 50 μ mol/l Gly-Pro-AMC, and buffer (100 mmol/l HEPES, pH 7.5, 0.1 mg/ml BSA) in a total reaction volume of 100 μ l. Liberation of AMC was monitored using an excitation wavelength of 360 nm and an emission wavelength of 460 nm. The enzyme used in these studies was soluble human protein produced in a baculovirus expression system (Bac-To-Bac; Life Technologies).

DPP8. Compounds were tested against human DPP8 (baculovirus) in a continuous fluorescent assay in 50 mmol/l sodium phosphate buffer, pH 8.0, and 0.1 mg/ml BSA, using Ala-Pro-7-amino-4-trifluoromethylcoumarin as substrate at 100 μ mol/l at 37°C for 15 min (excitation/emission: 400/505 nm).

DPP9. Compounds were tested against human DPP9 (baculovirus) in a continuous fluorescent assay in 100 mmol/l Tris/HCl buffer, pH 7.4, and 0.1 mg/ml BSA, using Gly-Pro-AMC as substrate at 100 μ mol/l at 37°C for 30 min (excitation/emission: 360/460 nm).

QPP. Compounds were tested against human QPP (baculovirus) in a continuous fluorescent assay in 100 mmol/l cacodylate buffer, pH 5.5, and 0.1 mg/ml BSA, using Nle-Pro-AMC as substrate at 5 μ mol/l at 37°C for 15 min (excitation/emission: 360/460 nm).

Fibroblast activation protein. Compounds were tested against human fibroblast activation protein (Glu₄₃₇ \rightarrow Gly mutant) (baculovirus) in a continuous fluorescent assay in 100 mmol/l Tris/HCl buffer, pH 8.0, 150 mmol/l NaCl,

and 0.1 mg/ml BSA, using Nle-Pro-AMC as substrate at 50 μ mol/l at 37°C for 15 min (excitation/emission: 360/460 nm).

Aminopeptidase P. Compounds were tested against human aminopeptidase P (*E. coli*) in a continuous fluorescent assay in 40 mmol/l Tris/HCl buffer, pH 7.4, 0.1 mg/ml BSA, 50 mmol/l NaCl, and 1 mmol/l MnCl₂, using Lys(Abz)Pro-Pro-pNA as substrate at 40 μ mol/l at 37°C for 30 min (excitation/emission: 310/410 nm).

Prolyl endopeptidase. Compounds were tested against human prolyl endopeptidase (*E. coli*) in a continuous fluorescent assay in 100 mmol/l sodium phosphate buffer, pH 7.5, 0.1 mg/ml BSA, 1 mmol/l EDTA, 5 mmol/l fresh dithiothreitol, and 100 mmol/l NaCl, using Z-Gly-Pro-AMC as substrate at 50 μ mol/l at 37°C for 30 min (excitation/emission: 360/460 nm).

Prolidase. Compounds were tested against prolidase from porcine kidney (Biozyme Laboratories) in a continuous UV/Vis assay in 50 mmol/l Tris/HCl buffer, pH 8.0, using 10 mmol/l Gly-Pro as substrate at 10 mmol/l at 37°C for 15 min (absorption monitored at 230 nm).

Data analysis. To measure the inhibition constants, serial dilutions of inhibitor were added to reactions containing enzyme and substrate. IC₅₀ values were determined by a fit of the reaction rates to a three-parameter Hill equation by nonlinear regression. To determine the dissociation constants (*K_i*), reaction rates were fit by nonlinear regression to the Michaelis-Menton equation for competitive, reversible inhibition.

In vitro assays for T-cell activation. Human peripheral blood mononuclear cells were isolated from healthy volunteers and stimulated overnight with either 10 μ g/ml phytohemagglutinin or with a mixture containing 100 pg/ml each of staphylococcal enterotoxins A, B, C1, D, and E (Toxin Technologies). Interleukin (IL)-2 concentrations in the culture supernatant were measured by immunoassay. Cell proliferation was measured by addition of 1 μ Ci ³H-thymidine followed by an overnight culture.

Oral glucose tolerance test in diet-induced obese mice. Male C57BL/6 mice (6–8 weeks of age) were obtained from Taconic Farms (Germantown, NY). Mice were fed a lean (control group) or high-fat (DIO group) diet (5 and 35% fat by weight, respectively) for 6–9 weeks and then administered an oral glucose tolerance test. Fasted DIO mice were orally dosed with vehicle (0.5% methylcellulose), compound 1, or compound 2 at 3, 10, or 30 mg/kg, 1 h before glucose (2 g/kg) challenge. Blood glucose was determined at various time points from tail bleeds using a glucometer.

Rat toxicity studies. CrI:CD(SD)IGS BR rats ~3–4 weeks of age were obtained from Charles River Laboratories, Wilmington, NC. At 6 weeks of age, rats (five rats per sex per group) were administered vehicle (0.5% methylcellulose) or compound (10, 30, and 100 mg \cdot kg⁻¹ \cdot day⁻¹) by oral gavage (5 ml/kg). Animals were observed daily for physical signs of toxicity. During the 2nd week of dosing, all rats were anesthetized with isoflurane, and blood samples were taken for determination of complete blood counts. In addition, serum samples from fasted rats were analyzed for a complete panel of clinical chemistry parameters. Urine was collected overnight for routine urinalysis. At termination of the study, all rats were killed, and a complete necropsy was conducted. An extensive list of tissues were dissected from all rats, weighed, fixed in 10% neutral buffered formalin, and processed by routine histology methods for microscopic examination.

Acute dog tolerability studies. Purpose-bred Beagle dogs were obtained from Marshall Farms, North Rose, NY. All dogs were acclimated for at least 4 weeks before study initiation. All compounds were formulated as aqueous suspensions in 0.5% methylcellulose and orally administered via gavage at a dose volume of 5 ml/kg. Following oral dosing, all animals were observed for several hours at frequent intervals and clinical signs of toxicity recorded for each dog.

Two-week toxicity study conducted in DPP-IV-deficient mice. Male and female DPP-IV-deficient (4) and wild-type (C57BL/6) mice were obtained at 6 weeks of age from Taconic Farms and acclimated for 2 weeks before the initiation of dosing. DPP-IV-deficient mice (six mice per sex per group) were administered vehicle (0.25% methylcellulose) or the DPP8/9-selective inhibitor (30, 100, and 300 mg \cdot kg⁻¹ \cdot day⁻¹) via oral gavage (5 ml/kg). Wild-type mice were administered compound at 300 mg \cdot kg⁻¹ \cdot day⁻¹. Animals were observed daily for physical signs of toxicity. At the completion of the 2-week study, a terminal blood sample was collected by cardiac puncture for complete blood counts. A necropsy was conducted and liver and spleen organ weight were recorded. Selected tissues were fixed in 10% neutral buffered formalin and processed by routine histology methods for microscopic examination. Tissue sections from all control and treatment groups were evaluated.

All *in vivo* procedures described above were conducted in laboratories accredited by AAALAC (Association for the Assessment and Accreditation of Laboratory Animal Care) International. All experimental protocols were approved by the Institutional Animal Care and Use Committee of Merck Research Laboratories.

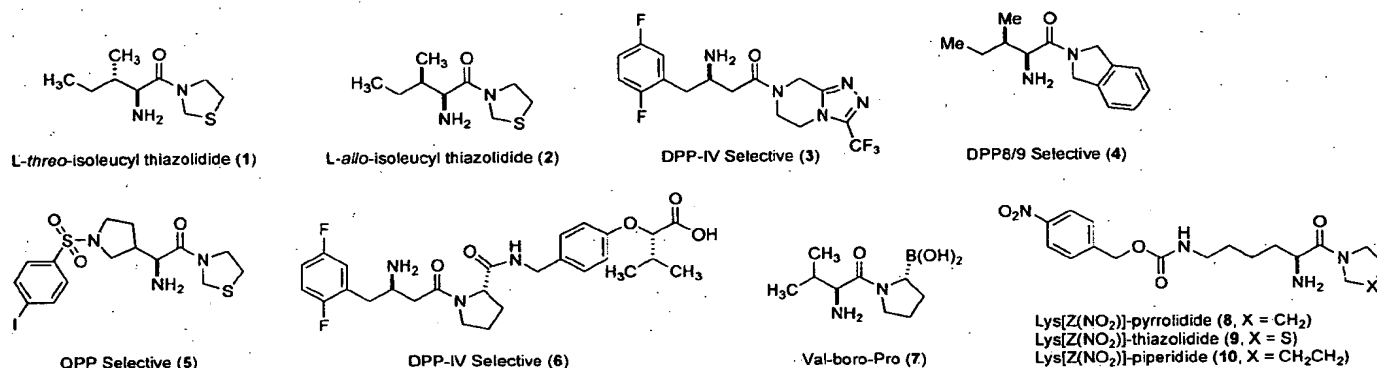


FIG. 1. Structures of compounds used in this study.

RESULTS

Preclinical toxicities of threo and allo isomers of isoleucyl thiazolidine. Several inhibitors of DPP-IV have been described (22). One representative example is L-threo-isoleucyl thiazolidine 1 (Fig. 1, compound 1) a DPP-IV inhibitor that has demonstrated efficacy in several animal models of diabetes (23–26). To evaluate the safety of this compound in preclinical species, 4-week toxicity studies in rats and dogs were conducted. In rats, toxicities were limited to the presence of lung histiocytosis and thrombocytopenia at relatively high doses (77.5 and 698 mg/kg, respectively). In dogs, acute central nervous system toxicities, characterized by ataxia, seizures, convulsions, and tremor, were observed at a dose of 75 mg/kg after one or two doses. Bloody diarrhea was observed at 225 mg/kg. No additional toxicities were observed upon dosing for 4 weeks. However, in subsequent chronic toxicity studies, upon 5–6 weeks of treatment with this compound in dogs, mortality and profound toxicities occurred at doses $\geq 25 \text{ mg} \cdot \text{kg}^{-1} \cdot \text{day}^{-1}$. These toxicities included anemia, thrombocytopenia, splenomegaly, and multiple organ pathology, mainly affecting the lymphoid system and gastrointestinal tract (Table 1).

The *allo* isomer of isoleucyl thiazolidine, compound 2, when compared with the *threo* isomer, has virtually identical

affinity to DPP-IV (Fig. 2A), similar pharmacokinetic (Table 2) and metabolic profiles (21), and similar in vivo efficacy in an oral glucose tolerance test in diet-induced obese mice (Fig. 2B). This compound was evaluated in 4-week toxicity studies in rats and acute tolerability studies in dogs. Although the toxicity profiles of the two compounds are qualitatively similar in both rats and dogs, the *allo* isomer was ~ 10 -fold more toxic when compared on either a dose level or plasma exposure basis (Table 1). In view of the comparable pharmacodynamic activity and pharmacokinetics in both species (Fig. 2 and Table 2), these results suggested that the toxicities were likely not due to DPP-IV inhibition but instead were potentially due to off-target activity. Evidence that these toxicities might be due to the inhibition of one or more proline-specific dipeptidyl peptidases was provided by studies with tissue extracts from DPP-IV-deficient mice. Detergent-solubilized extracts from the kidneys, liver, lung, and gastrointestinal tract of these animals were found to contain low levels of a proline-specific dipeptidyl peptidase activity, detected using the fluorogenic substrate Gly-Pro-AMC. The proline-selective dipeptidase activity in DPP-IV-deficient mice was 10- to 25-fold lower than that measured in corresponding tissues of wild-type animals and, unlike DPP-IV, was differentially inhibited by *threo* and *allo* isoleucyl thiazolidine ($\text{IC}_{50} = 726$ and 86 nmol/l , respectively). The 8.5-fold greater potency of the *allo* diastereomer against this activity suggested that off-target inhibition of one or more DPP-IV-like peptidases by this inhibitor could be responsible for preclinical toxicity.

Selectivity of threo- and allo-isoleucyl thiazolidines. The selectivity of the *threo* and *allo* isomers was determined in activity assays against a panel of diverse proteases, including DPP-IV-related peptidases. The compounds were also screened by MDS Pharma Services (PanLabs) in a panel of 170 receptor and enzyme assays. No significant activity ($\text{IC}_{50} < 100 \text{ } \mu\text{mol/l}$) was observed in any of the PanLabs assays, with the exception of the sigma σ_1 receptor for the *allo* compound ($K_i = 42 \text{ } \mu\text{mol/l}$). IC_{50} s $> 100 \text{ } \mu\text{mol/l}$ were observed for inhibition of several other proteases (cathepsins B and H, HIV protease, caspases 1–3 and 13, granzyme B, chymotrypsin, β and γ secretases, thrombin, trypsin, factor Xa, plasmin, tissue plasminogen activator, activated protein C, plasma kallikrein, and urokinase). For DPP-IV-related dipeptidyl peptidases (Table 3), inhibition was only observed for DPP-IV and the related dipeptidyl peptidases, QPP, DPP8, and DPP9. Inhibition of DPP8 and QPP by isoleucyl thiazolidine has been previously reported (27). Comparable QPP inhibition

TABLE 1
Preclinical toxicities of *allo*- and *threo*-isoleucyl thiazolidine

Species	Toxicity	<i>Threo</i> (mg/kg)	<i>Allo</i> (mg/kg)
Rat	Lung histiocytosis	77.5	10
	Thrombocytopenia	698	10
	Anemia	neg @ 698	100
	Splenomegaly/ lymphadenopathy	neg @ 698	10
	Mortality with multiple organ pathology	neg @ 698	300
Dog	Acute gastrointestinal toxicity	225	10
	Acute central nervous system toxicity	75	NT
	Thrombocytopenia	25	NT
	Anemia	25	NT
	Splenomegaly/ lymphadenopathy	25	NT
	Mortality with multiple organ pathology	75	NT

neg, negative finding at indicated dose; NT, not tested.

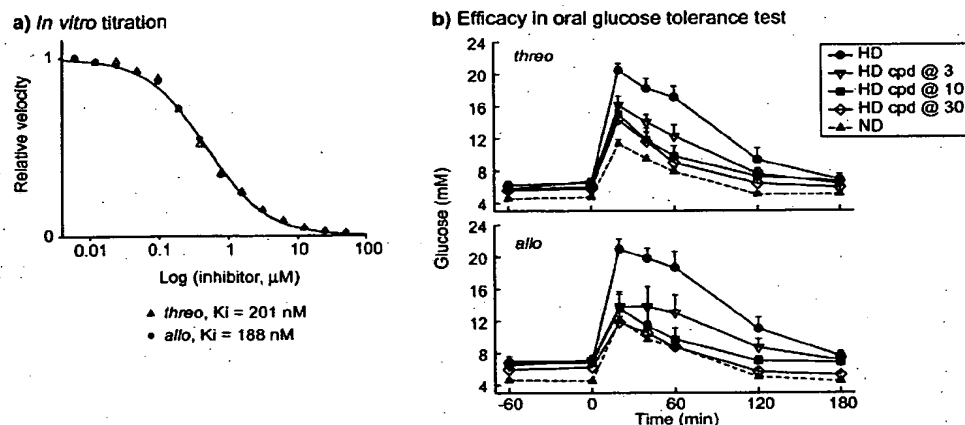


FIG. 2. In vitro and in vivo evaluation of *threo* and *allo* isomers of isoleucyl thiazolidine. **A:** *Threo*- and *allo*-isoleucyl thiazolidine were titrated against DPP-IV in an in vitro assay as described in RESEARCH DESIGN AND METHODS, and dissociation constants (K_i) were determined. The solid line is theoretical for K_i values for *threo* and *allo* of 201 and 188 nmol/l, respectively, indicating that both compounds bind to the enzyme with virtually identical affinity. **B:** *Threo*- and *allo*-isoleucyl thiazolidine were tested in an oral glucose tolerance test in high-fat diet-induced obese (DIO group) mice (HD, high fat diet; ND, normal diet). Treatment with single oral doses of 3, 10, or 30 mg/kg improved glucose tolerance in a dose-dependent manner. The area under the curve values in the treated groups were significantly less than in the vehicle control, and similar efficacy was observed with both compounds.

activity was observed for both isomers; however, the potency for inhibition of DPP8 and DPP9 differed by ~10-fold, with the *allo* isomer being more potent in each case. Since these differences in inhibition of DPP8/DPP9 were consistent with the observed differences in dose necessary to produce toxicity, it was hypothesized that inhibition of DPP8 and/or DPP9 was responsible for the observed toxicities of both compounds in preclinical species.

Identification of inhibitors selective for DPP-IV, DPP8/9, and QPP. Inhibitors selective for DPP-IV, QPP, and DPP8/9 were identified and their pharmacokinetic properties determined (Fig. 1 and Tables 2 and 3). The DPP-IV-selective compound 3 is a des-fluoro analog of DPP-IV inhibitor sitagliptin currently undergoing clinical investigation for the treatment of type 2 diabetes (28). This compound is a 27-nmol/l inhibitor of DPP-IV, with >1,000-fold selectivity over related proline-specific dipeptidyl peptidases. While potent and selective inhibitors of DPP8 and DPP9 have not been identified, a dual inhibitor, *allo*-isoleucyl isindoline derivative 4, was discovered. This compound has IC_{50} values of 38 and 55 nmol/l for

DPP8 and DPP9, respectively, and IC_{50} values >10 $\mu\text{mol/l}$ over the other related peptidases. QPP-selective inhibitor 5 (QPP $\text{IC}_{50} = 19 \text{ nmol/l}$) is 100- and 550-fold selective over DPP-IV and DPP9, respectively, and >1,000-fold selective over the remaining proline-specific dipeptidyl peptidases.

All three compounds are orally bioavailable in rats (Table 2), with half-lives ranging from ~0.5 to 2.5 h. Following oral administration at 2 mg/kg, similar exposures were observed for the DPP-IV-selective inhibitor 3 and QPP-selective inhibitor 5. At a similar dose level, the area under the curve observed for the DPP8/9-selective inhibitor 4 was approximately sevenfold higher. Further, the exposures observed for the DPP8/9-selective inhibitor 4 after a 10- and a 30-mg/kg dose were comparable to those observed after a 30- and 100-mg/kg dose of the DPP-IV-selective inhibitor 3. The C_{max} values of the DPP-IV inhibitor 3 and the DPP8/9 inhibitor 4 were similar following oral administration of 10, 30, and 100 mg/kg.

Toxicity studies with DPP-IV, QPP, and DPP-8/9 inhibitors in rats. To obtain evidence that DPP8/9 inhibition was responsible for the toxicities observed with the

TABLE 2

Pharmacokinetic properties of the *threo* and *allo* isomers of isoleucyl thiazolidine in rats and dogs (1 mg/kg i.v. and 2 mg/kg p.o.)

Species	Isomer	Cl_p ($\text{ml} \cdot \text{min}^{-1} \cdot \text{kg}^{-1}$)	Vd_{ss} (l/kg)	$t_{1/2}$ (h)	p.o. AUC ($\mu\text{mol} \cdot \text{l}^{-1} \cdot \text{h}^{-1}$)	C_{max} ($\mu\text{mol/l}$)	F (%)
Rat	<i>threo</i>	27	5.0	1.8	6.17	0.77	102
	<i>allo</i>	28	3.1	1.8	4.29	0.70	71
Dog	<i>threo</i>	33	2.2	1.4	4.19	0.44	84
	<i>allo</i>	29	2.4	1.0	2.34	0.40	80

Pharmacokinetic properties of selective compounds in rats

Compound	Dose (mg/kg)	Cl_p ($\text{ml} \cdot \text{min}^{-1} \cdot \text{kg}^{-1}$)	Vd_{ss} (l/kg)	$t_{1/2}$ (h)	p.o. AUC ($\mu\text{mol} \cdot \text{l}^{-1} \cdot \text{h}^{-1}$)	C_{max} ($\mu\text{mol/l}$)	F (%)
DPP-IV selective (3)	1 i.v., 2 p.o.	43	4.4	1.6	1.03	0.19	51
	10 p.o.				5.76	2.12	
	30 p.o.				26.7	10.7	
	100 p.o.				80.5	27.3	
DPP8/9 selective (4)	1 i.v., 2 p.o.	15	2.6	2.5	6.83	1.50	72
	10 p.o.				26.4	5.68	
	30 p.o.				91.1	15.6	
	100 p.o.				278	36.5	
QPP selective (5)	1 i.v., 2 p.o.	26	0.8	0.5*	1.17	0.78	45

*Mean residence time; $t_{1/2}$ could not be determined due to nonlinear kinetics.

TABLE 3
Selectivity of compounds for DPP-IV and related dipeptidyl peptidases

Compound	IC ₅₀ (nmol/l)							
	DPP-IV	DPP8	DPP9	QPP	FAP	PEP	APP	Prolidase
threo-Ile thia (1)	420	2,180	1,600	14,000	>100,000	>100,000	>100,000	>100,000
allo-Ile thia (2)	460	220	320	18,000	>100,000	>100,000	>100,000	>100,000
DPP-IV selective (3)	27	69,000	>100,000	>100,000	>100,000	>100,000	>100,000	>100,000
DPP8/9 selective (4)	30,000	38	55	14,000	>100,000	>100,000	>100,000	>100,000
QPP selective (5)	1,900	22,000	11,000	19	>100,000	63,000	>100,000	>100,000
DPP-IV selective (6)	0.48	>100,000	86,000	>100,000	21,000	39,000	>100,000	>100,000
Val-Boro-Pro (7)	<4	4	11	310	560	390	>100,000	>100,000
Lys[Z(NO ₂)] pyrrolidide (8)	1,300	154	165	1,210	51,000	>100,000	>100,000	>100,000
Lys[Z(NO ₂)] thiazolidide (9)	410	210	75	210	33,000	56,000	ND	>100,000
Lys[Z(NO ₂)] piperidide (10)	17,000	1,100	670	710	>100,000	>100,000	ND	ND

APP, aminopeptidase P; FAP, fibroblast activation protein; ND, not determined; PEP, prolyl endopeptidase.

allo and *threo* isomers, DPP-IV-, QPP-, and DPP8/9-selective compounds were evaluated in 2-week rat toxicity studies and in acute dog tolerability studies. The results from these studies showed a remarkable similarity between the effects produced by the DPP8/DPP9-selective inhibitor and the *allo* compound. As shown in Table 4, both compounds administered to rats produced mortality and a ventral, abdominal alopecia at similar doses. Both compounds also produced thrombocytopenia of similar magnitude at doses ≥ 30 mg/kg and enlarged spleens and lymph nodes at all doses tested. Although the *allo* compound produced anemia after 2 weeks of treatment that progressed in severity after 4 weeks of treatment, no anemia was observed with the DPP8/9-selective compound after 2 weeks; however, a reduction in reticulocyte counts was found in the 30- and 100-mg/kg dose groups (reticulocyte counts were not measured in the study with the *allo* compound). These data suggest that both compounds have an effect on hematopoiesis in the rat, possibly mediated by a protease other than DPP8/9. Alternatively, the compounds may have differential tissue distributions. Histologically, both compounds produced necrosis of lymphocytes within the spleen and lymph nodes. In addition, histiocytosis in the lungs and inflammatory cell infiltration of multiple organs, including the gastrointestinal tract, were observed.

The QPP-selective inhibitor produced significant reductions in reticulocyte counts at the 100-mg/kg dose. No other antemortem or postmortem changes were noted with this compound. The DPP-IV-selective inhibitor did not produce any changes in physical appearance, body

weight, hematology, clinical chemistry, urinalysis, ophthalmology, or postmortem changes in rats. Single-dose toxicokinetic data obtained at doses comparable to those used in the 2-week rat study show that exposures to the DPP-IV-selective compound were similar to, or greater than, the exposures of the *allo* compound associated with the above described toxicity.

Toxicity studies with DPP-IV, QPP, and DPP-8/9 inhibitors in dogs. Acute oral administration of the DPP8/DPP9-selective inhibitor resulted in bloody diarrhea, emesis, and tenesmus, similar to what had been previously observed with the *allo* compound. Conversely, no acute effects were observed in dogs given the DPP-IV-selective inhibitor, despite achieving plasma C_{max} and area under the curve values equal to or greater than those associated with the toxicity with the *allo* compound. No toxicity was observed in dogs given single oral doses of the QPP-selective inhibitor.

Studies with DPP8/9-selective inhibitor in DPP-IV-deficient mice. To demonstrate that the observed toxicities induced by the *allo* and DPP8/9-selective compounds were not due to residual DPP-IV inhibition, the DPP8/9-selective inhibitor was evaluated for toxicity in a 14-day tolerability study in wild-type and DPP-IV-deficient mice. The results are summarized in Table 5. Both 300-mg \cdot kg⁻¹ \cdot day⁻¹ dose groups were terminated due to excessive mortality and clinical signs of morbidity, indicating that these findings were not due to inhibition of DPP-IV. Findings in DPP-IV-deficient mice at 100 mg \cdot kg⁻¹ \cdot day⁻¹ included splenomegaly, increased extramedullary hematopoiesis in the spleen, and bone marrow myeloid hyperpla-

TABLE 4
Comparative toxicity studies in rats (2 weeks of treatment at doses of 10, 30, 100 mg \cdot kg⁻¹ \cdot day⁻¹) and dogs (single dose, 10 mg/kg p.o.) with selective inhibitors

Species	Toxicity	DPP-IV selective (3) (mg/kg)	DPP8/9 selective (4) (mg/kg)	QPP selective (5) (mg/kg)	threo-Ile thia (1) (mg/kg)	allo-Ile thia (2) (mg/kg)
Rat	Alopecia	NO	100 (5/10)	NO	NO	100 (2/10)
	Thrombocytopenia	NO	30 (3/10)	NO	675 (10/20)	10 (2/10)
	Anemia	NO	NO	NO	NO	100 (5/20)
	Reticulocytopenia	NO	30 (2/10)	100 (1/5)	NO	ND
	Splenomegaly	NO	10 (4/10)	NO	NO	10 (7/10)
	Mortality	NO	100 (2/10)	NO	NO	300 (7/10)
Dog	Bloody diarrhea	NO	10 (3/3)	NO	225 (1/6)	10 (3/3)

The lowest dose producing the adverse effect is shown with the incidence at this dose in parentheses. Historical data from threo- and allo isoleucyl-thiazolidine safety studies are shown for comparison. NO, not observed at any dose tested; ND, not determined.

TABLE 5
Comparative toxicity studies with the DPP8/9-selective inhibitor (4) in wild-type and DPP-IV-deficient mice

Toxicity	DPP-IV-deficient mice (mg/kg)	Wild-type mice (mg/kg)
Spleen (EMH)	30 (2/12); 100 (11/12)	ND
Bone marrow myeloid hyperplasia	100 (7/12)	ND
Mortality	100 (1/12); 300 (12/12)	300 (12/12)

Wild-type mice ($300 \text{ mg} \cdot \text{kg}^{-1} \cdot \text{day}^{-1}$ p.o.) and DPP-IV-deficient mice (30, 100, and $300 \text{ mg} \cdot \text{kg}^{-1} \cdot \text{day}^{-1}$ p.o.) were treated for 2 weeks. The dose(s) producing the adverse effect is shown with the incidence in parenthesis. EMH, extramedullary hematopoiesis; ND, not determined.

sia; these findings were also observed in rats treated with the DPP8/9 selectivity inhibitor, as described above.

Studies with DPP-IV-, DPP8/9-, and QPP-selective inhibitors in in vitro models of T-cell activation. Lys[Z(NO₂)]-pyrrolidine (compound 8) and related compounds 9 and 10 (Fig. 1) that have been previously used to implicate DPP-IV activity in T-cell activation were found to be nonselective DPP-IV inhibitors, with $\text{IC}_{50\text{s}} < 1 \text{ } \mu\text{mol/l}$ for DPP8/9 (Table 3), raising the possibility that some of the reported effects of these compounds were due to off-target activity. To test this hypothesis, QPP- and DPP8/9-selective inhibitors (compounds 5 and 4, respectively), a potent nonselective inhibitor, Val-boro-Pro (compound 7), and one of the most potent and selective DPP-IV inhibitors discovered to date (Fig. 1, compound 6) (29), were tested in in vitro models of immune responses. Effects on proliferation and IL-2 release of human T-cells upon both phytohemagglutinin and superantigen stimulation were determined. Val-boro-Pro and the selective DPP8/9 inhibitor inhibited proliferation in these models with $\text{IC}_{50\text{s}}$ of ~ 10 and 500 nmol/l , respectively (Fig. 3). Val-boro-Pro also inhibited IL-2 release in these models with an IC_{50} $\sim 500 \text{ nmol/l}$ (not shown). In contrast, the QPP (data not shown)- and DPP-IV-selective compounds had no effect in these assays ($\text{IC}_{50} > 50 \text{ } \mu\text{mol/l}$).

DISCUSSION

There is evidence from preclinical studies in animal models of diabetes, studies of DPP-IV-deficient mice, and from clinical studies of DPP-IV inhibitors indicating potential utility of DPP-IV inhibition for the treatment of patients with type 2 diabetes. With the recent identification of several closely related proline-specific enzymes, understanding the degree of selectivity required for the development of inhibitors with an optimal safety profile has become a key issue. The data presented in this manuscript provide compelling evidence that inhibition of DPP8/9, but not selective DPP-IV inhibition, is associated with multi-organ toxicities in preclinical species.

First, at least two structurally distinct compounds that inhibit DPP8/9 show remarkably similar toxicities in rats and dogs. The DPP8/9 inhibitor is highly selective over all other proline specific enzymes, and inhibition of the *allo* compound is limited to DPP-IV, DPP8/9, and weak inhibition of QPP. The finding that the DPP8/9 inhibitors produce similar toxicities in DPP-IV-deficient and wild-type mice establishes that the observed toxicities are not due to inhibition of DPP-IV. Second, the degree of toxicity ob-

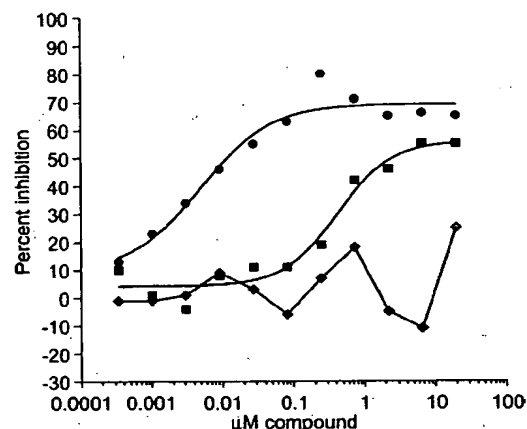


FIG. 3. Effects of selective inhibitors on proliferation of human peripheral blood mononuclear cells. Val-boro-Pro (●), DPP8/9-selective inhibitor 4 (■), and DPP-IV-selective inhibitor 6 (◆) were tested in human peripheral blood mononuclear cells for effects on proliferation. Cells were stimulated with either phytohemagglutinin or superantigen (shown). Val-boro-Pro and the selective DPP8/9 compound inhibited proliferation in this model with $\text{IC}_{50\text{s}}$ of ~ 10 and 500 nmol/l , respectively. The DPP-IV inhibitor had no effect in these assays ($\text{IC}_{50} > 50 \text{ } \mu\text{mol/l}$).

served with the *allo* and *threo* compounds correlates with their affinity for DPP8/9. No other distinguishing characteristics for these two isomers that could explain their differential toxicity have been identified. Third, gastrointestinal toxicity in the dog has been reported following oral administration of another DPP-IV inhibitor, CP-867534-01 [(S)-2-amino-2-cyclohexyl-1-(3,3,4,4-tetrafluoropyrrolidin-1-yl)ethanone hydrochloride] (30). We have found that this compound also inhibits DPP8 and DPP9 with $\text{IC}_{50\text{s}} < 100 \text{ nmol/l}$. Taken together, these findings strongly suggest that DPP8/9 inhibition results in toxicity in preclinical species, although they do not unequivocally rule out the possible contribution of other closely related enzymes. The molecular mechanism that underlies the observed toxicities is unknown.

One theoretical liability of DPP-IV inhibition is compromised immune function because DPP-IV is identical to CD26, a cell surface marker for activated T-cells (19). Indeed, there has been an intense effort to establish whether the catalytic activity of DPP-IV is required for T-cell activation, in part, using inhibitors of DPP-IV, which attenuate T-cell activation in a variety of models of immune function (20). We now report that the compounds used in these experiments have greater intrinsic potency against DPP8 and DPP9 than DPP-IV. Moreover, the DPP8/9-selective inhibitor (compound 4), but not the selective DPP-IV inhibitor (compound 6), attenuated proliferation and IL-2 release in human in vitro models of T-cell activation. These results strongly suggest that proteolytic activity is not required for the putative costimulatory function of DPP-IV/CD26 and that immunological effects previously observed with several DPP-IV inhibitor compounds in preclinical models may be due to off-target inhibition of DPP8/9.

These results do not establish whether inhibition of DPP8 or DPP9 (or both) is more important in producing toxicity. Of note, DPP8/9 are cytosolic enzymes, in contrast to DPP-IV, which has an extracellular catalytic domain. Thus, for a given compound, the potential for toxicities at efficacious doses will depend not only upon

the intrinsic potency against DPP8 and/or DPP9 relative to DPP-IV but also on the intracellular concentration achieved. Indeed, the *threo* and *allo* isomers, and the DPP8/9 inhibitor, are highly cell penetrant. Also unknown is the extent to which the toxicities observed in preclinical species will extend to humans. Given the high degree of homology of DPP8 and DPP9 across species, and the finding that a selective DPP8/9 inhibitor attenuates T-cell activation in a human in vitro system, it is reasonable to speculate that some liabilities of DPP8/9 inhibition may be observed in humans, provided inhibition of these enzymes occurs in vivo.

In summary, these results strongly suggest that inhibition of DPP8/9 produces profound toxicity in preclinical species and is also likely responsible for at least some of the effects on immune function that have been previously attributed to DPP-IV. Some of the toxicities that were noted in dogs did not manifest until 5–6 weeks of treatment, indicating that relatively long-term inhibition of these enzymes may be required to properly assess potential liabilities of DPP8/9 inhibition. Conversely, no toxicities or attenuation of T-cell activation in vitro were observed with selective DPP-IV inhibitors in these studies or in rats and dogs treated for 12 months at doses well above those necessary for pharmacological activity (G.R.L., unpublished data). Taken together, these results strongly suggest that early preclinical assessment of potential clinical candidates for off-target peptidase inhibition is important, with selection and further development of agents that have essentially no DPP8/9 inhibition at pharmacologically relevant plasma exposures.

ACKNOWLEDGMENTS

The authors are indebted to Hans-Ulrich Demuth (probiotic AG) for providing results from the 4-week rat study with *L-threo*-isoleucyl thiazolidine (compound 1). The manuscript is dedicated to the memory of Barbara Leiting.

REFERENCES

- Deacon CF, Ahrén B, Holst J: Inhibitors of dipeptidyl peptidase IV: a novel approach for the prevention and treatment of type 2 diabetes? *Expert Opin Investig Drugs* 13:1091–1102, 2004
- Ahrén B, Landin-Olsson M, Jansson PA, Svensson M, Holmes D, Schweizer A: Inhibition of dipeptidyl peptidase-4 reduces glycemia, sustains insulin levels, and reduces glucagon levels in type 2 diabetes. *J Clin Endocrinol Metab* 89:2078–2084, 2004
- Ahrén B, Gomis R, Standl E, Mills D, Schweizer A: Twelve- and 52-week efficacy of the dipeptidyl peptidase IV inhibitor LAF237 in metformin-treated patients with type 2 diabetes. *Diabetes Care* 27:2874–2880, 2004
- Marguet D, Baggio L, Kobayashi T, Bernard AM, Pierres M, Nielsen PF, Ribet U, Watanabe T, Drucker DJ, Wagtmann N: Enhanced insulin secretion and improved glucose tolerance in mice lacking CD26. *Proc Natl Acad Sci* 97:6874–6879, 2000
- Conarello SL, Li Z, Ronan J, Roy RS, Zhu L, Jiang G, Liu F, Woods J, Zychband E, Moller DE, Thornberry NA, Zhang BB: Mice lacking dipeptidyl peptidase IV are protected against obesity and insulin resistance. *Proc Natl Acad Sci* 100:6825–6830, 2003
- Drucker DJ: Enhancing incretin action for the treatment of type 2 diabetes. *Diabetes Care* 26:2929–2940, 2003
- Zander M, Madsbad S, Madsen JL, Holst JJ: Effect of 6-week course of glucagon-like peptide 1 on glycaemic control, insulin sensitivity, and β -cell function in type 2 diabetes: a parallel-group study. *Lancet* 359:824–830, 2002
- Kieffer TJ, McIntosh CHS, Pederson TA: Degradation of glucose-dependent insulinotropic polypeptide and truncated glucagon-like peptide 1 in vitro and in vivo by dipeptidyl peptidase IV. *Endocrinol* 136:3585–3596, 1995
- Mentlein R, Gallwitz B, Schmidt WE: Dipeptidyl-peptidase IV hydrolyses gastric inhibitory polypeptide, glucagon-like peptide-1 (7–36)amide, peptide histidine methionine and is responsible for their degradation in human serum. *Eur J Biochem* 214:829–835, 1993
- Balkan B, Kwasnik L, Miserendino R, Holst JJ, Li X: Inhibition of dipeptidyl peptidase IV with NVP-DPP728 increases plasma GLP-1 (7–36 amide) concentrations and improves oral glucose tolerance in obese Zucker rats. *Diabetologia* 42:1324–1331, 1999
- Sedo A, Malik R: Dipeptidyl peptidase IV-like molecules: homologous proteins or homologous activities? *Biochim Biophys Acta* 1550:107–116, 2001
- Underwood R, Chiravuri H, Lee H, Schmitz R, Kabcenell AK, Yardley K, Huber BT: Sequence, purification, and cloning of an intracellular serine protease, quiescent cell proline dipeptidase. *J Biol Chem* 274:34053–34058, 1999
- Abbott CA, Yu CM, Woollatt E, Sutherland GR, McCaughan GW, Gorrell MD: Cloning, expression and chromosomal localization of a novel human dipeptidyl peptidase (DPP) IV homolog, DPP8. *Eur J Biochem* 267:6140–650, 2000
- Ajami K, Abbott CA, McCaughan W, Gorrell MD: Dipeptidyl peptidase 9 has two forms, a broad tissue distribution, cytoplasmic localization, and DP-IV-like peptidase activity. *Biochimica et Biophysica Acta* 1679:18–28, 2004
- Park JE, Lenter MC, Zimmermann RN, Garin-Chesa P, Old LJ, Rettig WJ: Fibroblast activation protein, a dual specificity serine protease expressed in reactive human tumor stromal fibroblasts. *J Biol Chem* 274:36505–36512, 1999
- Duke-Cohan JS, Gu J, McLaughlin DF, Xu Y, Freeman GJ, Schlossman SF: Attractin (DPPT-L), a member of the CUB family of cell adhesion and guidance proteins, is secreted by activated human T lymphocytes and modulates immune cell interactions. *Proc Natl Acad Sci* 95:11336–11341, 1998
- Blanco J, Jacotot E, Callebaut C, Krust B, Hovanessian AG: Dipeptidyl-peptidase IV- β : further characterization and comparison to dipeptidyl-peptidase IV activity of CD26. *Eur J Biochem* 256:369–378, 1998
- Chen W-T, Kelly T, Ghersi G: DP-IV, seprase, and related serine peptidases in multiple cellular functions. *Curr Topics Develop Biol* 54:207–232, 2003
- De Meester I, Korom S, Van Damme J, Scharpe S: CD26, let it cut or cut it down. *Immunology Today* 20:367–375, 1999
- Reinhold D, Kahne T, Steinbrecher A, Wrenger S, Neubert K, Ansorge S, Brocke S: The role of dipeptidyl peptidase IV (DP-IV) enzymatic activity in T cell activation and autoimmunity. *Biol Chem* 383:1133–1138, 2002
- Beconi MG, Mao A, Liu DQ, Kochansky C, Pereira T, Raab C, Pearson P, Lee Chiu SH: Metabolism and pharmacokinetics of a dipeptidyl peptidase IV inhibitor in rats, dogs, and monkeys with selective carbamoyl glucuronidation of the primary amine in dogs. *Drug Metab Dispos* 31:1269–1277, 2003
- Weber AE: Dipeptidyl peptidase IV inhibitors for the treatment of diabetes. *J Med Chem* 47:4135–4141, 2004
- Pospisilik JA, Stafford SG, Demuth HU, Brownsey R, Parkhouse W, Finegood DT, McIntosh CH, Pederson RA: Long-term treatment with dipeptidyl peptidase IV inhibitor P32/98 causes sustained improvements in glucose tolerance, insulin sensitivity, hyperinsulinemia, and β -cell responsiveness in VDF (*fa/fa*) Zucker rat. *Diabetes* 51:943–950, 2002
- Pauly RP, Demuth HU, Rosche R, Schmidt J, White HA, McIntosh CHS, Pederson RA: Inhibition of dipeptidyl peptidase IV (DP-IV) in rat results in improved glucose tolerance (Abstract). *Regul Pept* 64:148, 1996
- Pederson RA, White HA, Schlenzig D, Pauly RP, McIntosh CH, Demuth H-U: Improved glucose tolerance in Zucker fatty rats by oral administration of the dipeptidyl peptidase IV inhibitor isoleucine thiazolidine. *Diabetes* 47:1253–1258, 1998
- Pospisilik JA, Stafford SG, Demuth H-U, McIntosh CHS, Pederson RA: Long-term treatment with dipeptidyl peptidase IV inhibitor improves hepatic and peripheral insulin sensitivity in the VDF Zucker rat. *Diabetes* 51:2677–2683, 2002
- Jiang W, Chen Y, Hsu T, Wu S, Chien C, Chang C, Chang S, Lee S, Chen X: Novel isoindoline compounds for potent and selective inhibition of prolyl dipeptidase DPP8. *Bioorg Med Chem Letters* 15:687–691, 2005
- Kim D, Wang L, Beconi M, Eiermann GJ, Fisher MH, He H, Hickey GJ, Kowalchick JE, Leiting B, Lyons K, Marsilio F, McCann ME, Patel RA, Petrov A, Scapin G, Patel SB, Sinha Roy R, Wu JK, Wyvratt MJ, Zhang BB, Zhu L, Thornberry NA, Weber AE: (2R)-4-Oxo-4-[3-(trifluoromethyl)-5,6-dihydro[1,2,4]triazolo[4,3-a]pyrazin-7(8H)-yl]-1-(2,4,5-trifluorophenyl)butan-2-amine: a potent, orally active dipeptidyl peptidase IV inhibitor for the treatment of type 2 diabetes. *J Med Chem* 48:141–151, 2005
- Edmondson SD, Mastracchio A, Beconi M, Colwell LF, Habulihaz B, He H, Kumar S, Leiting B, Lyons KA, Mao A, Marsilio F, Patel RA, Wu JK, Zhu L, Thornberry NA, Weber AE, Parmee ER: Potent and selective proline derived dipeptidyl peptidase IV inhibitors. *Bioorg Med Chem Lett* 14:5151–5155, 2004
- Parker JC, Hulin B, Vanvolkenburg MA, Lopaze MG, Sagawa K, Ogorman MT, Gerdin K, Andrews KM, Brees DJ, Reagan WJ: A novel fluorinated cyclic amide inhibitor of dipeptidyl peptidase IV improves glucose tolerance in murine models of diabetes mellitus (Abstract). *Diabetes* 52 (Suppl. 1) (16-late-breaking abstract), 2003

Available online at www.sciencedirect.com

SCIENCE @ DIRECT®

Biochimica et Biophysica Acta 1679 (2004) 18–28

www.bba-direct.com

Dipeptidyl peptidase 9 has two forms, a broad tissue distribution, cytoplasmic localization and DPIV-like peptidase activity

Katerina Ajami^a, Catherine A. Abbott^b, Geoffrey W. McCaughan^a, Mark D. Gorrell^{a,*}

^a*A.W. Morrow Gastroenterology and Liver Centre, Royal Prince Alfred Hospital, Centenary Institute of Cancer Medicine and Cell Biology and The University of Sydney, Locked Bag No. 6, Newton, New South Wales 2042, Australia*

^b*School of Biological Sciences, Flinders University, Adelaide, South Australia, Australia*

Received 25 November 2003; received in revised form 24 March 2004; accepted 31 March 2004
Available online 27 April 2004

Abstract

Dipeptidyl peptidase (DP) IV has a distinct substrate specificity in hydrolyzing a post-proline bond. Here we present novel data on the sizes and tissue distribution of human and rat gene products and the peptidase activity of the DPIV-related gene DP9. A short cDNA of 2589 bp and a long cDNA of 3006 bp of DP9 were cloned. A ubiquitous predominant DP9 mRNA transcript at 4.4 kb represented the short form, whereas a less abundant 5.0-kb transcript present predominantly in muscle represented the long form. Both forms of DP9 have no transmembrane domain and two potential N-linked glycosylation sites. DP9 exhibited post-proline dipeptidyl aminopeptidase activity and was a cytoplasmic, 110-kDa monomer. Thus, the six DPIV gene family members have diverse characteristics: only DP9 and DP8 have exclusively cytoplasmic localization and only DP9, DP8, fibroblast activation protein (FAP) and DPIV have peptidase activity.
© 2004 Elsevier B.V. All rights reserved.

Keywords: Dipeptidyl peptidase; Prolyl oligopeptidase; Fibroblast activation protein; Gene expression; Serine proteinase; CD26

Few proteinases are capable of cleaving the post-proline bond and very few can cleave such a bond two positions from the N-terminus. The latter small subset of serine proteinases, the post-proline dipeptidyl aminopeptidases, consists of three enzymes of the dipeptidyl peptidase (DP) IV gene family. DPIV (E.C. 3.4.14.5), fibroblast activation protein (FAP) and DP8 [1], and DPLI [2] (E.C. 3.4.14.2).

DPIV is a ubiquitous, multifunctional homodimeric glycoprotein with roles in nutrition, metabolism, the immune and endocrine systems, cancer growth and cell adhesion [3–7]. Important DPIV substrates include many chemokines, neuropeptide Y, glucagon-like peptide-1 and glucose-dependent insulinotropic peptide. DPIV inhibitors are undergoing clinical trials as a new therapy for type 2 diabetes [4,8,9]. The DPIV gene family has six members including the two

non-enzymes DPL1 (DPP6/DPP-X) and DPL2 [1]. DPIV, FAP, DPL1 and DPL2 are type II cell surface glycoproteins of 760 to 865 amino acids. DPIV is widely expressed on lymphocytes as well as on endothelial and epithelial, including acinar, cells of a wide variety of tissues [3]. Low levels of DPIV (CD26) are found on resting lymphocytes, but its expression is strongly up-regulated following activation [10]. An additional soluble form of DPIV occurs in semen and serum [11]. FAP is not expressed in the adult except in locations of tissue remodelling, such as tumours and liver disease [12,13].

DPL1 has both long and short forms, of 865 and 803 amino acids, respectively, in which the additional residues lengthen the N-terminal cytoplasmic tail. The DPL1 long form is expressed in brain and pancreas whereas the DPL1 short form is in many organs, but not muscle, liver, spleen or heart [14,15]. DPL2 has five alternate transcripts including two with differing N-terminal cytoplasmic tails [16]. DPL2 expression is restricted primarily to brain, pancreas and adrenal [16–18]. DP8 has 882 amino acids and 26% amino acid identity with DPIV but differs from DPIV and FAP in being exclusively monomeric and cytoplasmic [19]. DP8 catalytic triad residues, Ser⁷³⁹–Asp⁸¹⁷–His⁸⁴⁹, and Glu²⁵⁹

Abbreviations: AFC, 7-Amido-4-trifluoromethylcoumarin; BLAST, Basic Local Alignment Search Tool; DP, dipeptidyl peptidase; DPL, DP-like; EST, expressed sequence tag; FAP, fibroblast activation protein; mAb, monoclonal antibody; NA, nitroanilide; PCR, polymerase chain reaction; PO, prolyl oligopeptidase; RACE, Rapid amplification of cDNA ends

* Corresponding author. Tel.: +61-2-95656152; fax: +61-2-95656101.

E-mail address: m.gorrell@centenary.usyd.edu.au (M.D. Gorrell).

are homologous to DPIV in both structure and function [20]. DP8 is ubiquitous and is up-regulated in activated T cells [18,19].

We identified human DP9 as a DPIV family member by its close sequence similarity to DP8, in genomic sequence [1]. Here we report our DP9 cDNA clones, enzyme function of recombinant DP9 and in vivo expression patterns of two alternatively spliced forms of the *DP9* gene in human and rat tissues.

1. Experimental procedures

1.1. Materials

The cDNAs used were CD26 [21], DP8 [19] and short and long DP9, which have GenBank™ accession numbers M80536, AF221634 and AY374518 and AF542510, respectively. Polymerase chain reaction (PCR) used Platinum Pfx DNA polymerase (Invitrogen, Carlsbad, CA, USA) or Advantage 2 Polymerase Mix (Clontech, Palo Alto, CA, USA). Plasmid DNA was extracted using either the Rapid Pure Miniprep Kit (Bio101, Vista, CA, USA) or the JET-STAR Plasmid Maxiprep Kit (GENOMED, Germany).

1.2. RNA isolation and cDNA synthesis

RNA was prepared from human T-cell line CEM (ATCC, CCL-119) and snap frozen human cirrhotic liver tissue, cDNA was synthesized using Superscript II reverse transcriptase (Invitrogen, Carlsbad, CA) and rapid amplification of cDNA ends (RACE) was performed as described previously [19].

1.3. Bioinformatics

Basic Local Alignment Search Tool nucleotide (BLASTn) analysis [22] was used to identify the *DP9* gene expressed sequence tags (ESTs) in GenBank and a BLAT was used to determine exon structure using the UCSC Genome Browser (<http://genome.ucsc.edu/>) [23]. Multiple sequence alignments and phylogenetic analysis were performed through the Australian National Genomic Information Service (ANGIS, Sydney, Australia) as described previously [19]. The AC005783 sequence was translated into three reading frames to seek putative exons containing a start codon.

1.4. Cloning full-length DP9 constructs

The sequences of AC005594 and AC00573 genomic clones were used to design the forward primer, DP9_*Xba*I_Foward (CGCGCGTCTAGAGGGCGGGATGCCTCACTGG) and the reverse primer DP9_*Xba*I_Reverse_Fusion (GGCCGCTCTAGAGAGGTATTCCTGTAGAAAGTG) for PCR from the CEM cell line cDNA.

The PCR conditions were 95 °C for 2 min, followed by 35 cycles of 95 °C for 15 s, 55 °C for 30 s and 68 °C for 1 min per kilobase (kb) of product. The *Xba*I/*Xba*I 2589 base pair (bp) cDNA of DP9 with an open reading frame of 863 amino acids was ligated into the *Xba*I-digested pcDNA3.1/V5/HisA vector. The stop codon in the DP9 expression construct in pcDNA3.1/V5/HisA was altered using PCR to create a C-terminal fusion with the V5 and His tag contained in the vector. DP9 genomic DNA sequence was used to design the forward primer, DP9_*Xba*I_Foward_Long (CGCGCGTCTAGACCTGAGCCGGCGGGTCC) and the reverse primer DP9_*Xba*I_Reverse_Fusion (as above) for PCR from the CEM cell line RNA. The *Xba*I/*Xba*I 2913 base pair (bp) cDNA of DP9 with a predicted open reading frame of 971 amino acids was ligated into the *Xba*I-digested pEF-BOS vector [24]. This construct was named pEF-BOS-DP9_Long. All expression constructs subcloned into pcDNA3.1/V5/His and pEF-BOS were verified by full sequence analysis.

1.5. DP9 gene expression in human and rat tissues

DP9 genomic sequence was used to design the forward primer, DP9_primer_3 (AAACTGGCTGAGTTCCA-GACTGAC) and the reverse primer DP9_primer_1 (GCTCAGAGGTATTCCTGTAGAAAG) to generate a 1.5-kb DP9 clone, which was used in synthesizing a 3' DP9 probe (1353–2898 nt). Forward primer DP9_primer_22 (GCCGCGGGTCCCTGTGTCCG) and reverse primer DP9_primer_28 (CCTCTCAGCCCCCTCGGAATTCAG) were used to generate a 306-bp DP9 clone, which was used in synthesizing a 5' DP9 probe (4–306 nt). Forward primer DP9_primer_MET (GGGATAAGAAGGATGAGATTCAAGGGC) and reverse primer DP9_primer_1 (GCTCAGAGGTATTCCTGTAGAAAG) were used to generate a 2618-bp DP9 clone, which was used in synthesizing a DP9 probe (295–2913 nt) and hybridised to a Rat Multiple Tissue Northern Blot (Clontech). The hybridisation was carried out overnight at 60 °C to allow for cross-species differences. The 1.5-kb PCR product was labelled with ³²P using a Megaprime™ Labelling Kit (Amersham Pharmacia Biotec, UK) and hybridised to a Master RNA blot (Clontech), Human Multiple Tissue Northern Blots I and II (Clontech) as described previously [19]. The 306-bp PCR product was labelled with ³²P, using a RediPrime II Labelling system (Amersham Pharmacia Biotec).

1.6. Transfection

Cultivation and transfection of the human kidney epithelial line 293T (ATCC, CRL-11268) and monkey kidney fibroblast (COS-7) cells (ATCC, CRL-1651) were carried out as described previously [1,20]. The presence of peptidase fused with the V5 epitope was detected using an anti-V5 monoclonal antibody (mAb) (Invitrogen, The Nether-

lands). Immunofluorescence cytochemistry, flow cytometry and immunoblotting were performed as described previously [13,19,20,25].

1.7. Enzyme assays

DPIV enzyme activity was measured at 37 °C as described previously [19,20] except that cells were diluted in phosphate buffered saline pH 7.4. DP9 was tested for its ability to hydrolyse 4 mM H-Ala-Pro-AFC, H-Gly-Pro-p-nitroanilide (NA) and H-Ala-Pro-4-methoxyβNA·HCl (Bachem, Bubendorf, Switzerland) [20]. Substrate was diluted in 0.1% Tween 20 to permeabilise the cells. Assays were done in triplicate.

2. Results

2.1. DP9 molecular cloning and sequence analysis

Two overlapping cosmids containing a novel DP8 homolog at 19p13.3 were identified using a BLASTn search into GenBank. A partial cDNA was predicted by joining the overlapping cosmids numbered R26894, accession number AC005594, and R33083, accession number AC005783 (Table 1). The novel protein was named dipeptidyl peptidase 9 in consultation with Professor Alan Barrett (MEROPS: the protease database; (<http://merops.sanger.ac.uk>) [26].

The two primers designed from the genomic clones, DP9_primer_3 and reverse primer DP9_primer_1, were used in reverse transcriptase-PCR to create a 1.5-kb product. The sequence of this product showed that approximately 50% of the DP9 exon–intron boundaries predicted by the *grail2*exons_human_1.3 algorithm were incorrect. Multiple rounds of RACE generated a cDNA that encoded 830 amino acids and lacked a start codon. The longest DP9 cDNA was generated using CEM cell RNA and primers DP9-*Xba*I_Foward_Long and DP9-*Xba*I_Reverse_Fusion. This PCR product had a 2913-bp ORF encoding 971 amino acids. The cloned DP9 was identical to the genomic sequence over these 2913 bp. The technique of 5' RACE using dC tailing did not contribute any further information. Extensive searches identified many ESTs containing sequences identical to the DP9 long form (Table 2) but none contained additional 5' sequence. Therefore, a start Met of the long form was not located.

Table 1
DP9 GenBank accession numbers

Genomic DNA cosmid number	R26894	R33083
Corresponding accession number	AC005594	AC005783
Cosmid size (bp)	39,514	43,501
cDNA (3006 bp) accession number	AF542510	
cDNA (2589 bp) accession number	AY374518	

Table 2
Human DP9 ESTs that contain sequence specific for the long form of DP9 cDNA

Tissue	Accession number ^a	Length (bp)
<i>Diseased tissue</i>		
Eye retinoblastoma	BU187663	909
Paediatric acute myelogenous leukemia	BM14674	564
Paediatric pre-B cell acute lymphoblastic leukemia	BE244612	383
Skin melanotic melanoma	BQ212416	927
Skin melanotic melanoma	BE727051	1169
Skin melanotic melanoma	BM560972	1077
Skin melanotic melanoma	BM558851	1000
Skin melanotic melanoma	BG334474	908
Placenta choriocarcinoma	BK336652	900
Neuroblastoma	AL519618	1201
Neuroblastoma	BX394449	1043
Neuroblastoma	AL529248	881
Lung large cell carcinoma	BQ957392	948
<i>Normal tissue</i>		
Ovary	BM544154	1087
Placenta	CB990269	817
Placenta	CB988911	797
Placenta	CB960267	739
Placenta	CD109577	774
Placenta	CB960490	757
Placenta	CB960096	808
Testis	BU164620	846
Leukocyte	BI911262	713
Leukocyte	BI910501	370
Stomach lymphoblast-like cell	BM799399	410
<i>Cell lines</i>		
Testis embryonic carcinoma cell line	BQ217800	968
B cell (Ramos cell line)	HX385217	1125
B cell (Ramos cell line)	BX364390	1201
T cell (Jurkat cell line)	BX443745	727
T cell (Jurkat cell line)	BX421701	1201

^a Identified by a BLASTn search of the GenBank EST database.

Our 3006-bp cDNA (AF542510) comprising 2913 bp of ORF plus 3' non-coding was used in a BLAT search at the UCSC Genome Browser on the Human April 2003 Freeze (<http://genome.ucsc.edu/>). This revealed a DP9 gene of 48.6 kb located on the negative strand at base 4,616,486 to 4,663,828 at 19p13.3. The short form of DP9 derives from 19 exons and the long form from 22 exons. The biological significance of the two forms is unknown. The extra 5' sequence is either coding or 5' non-coding sequence. In approximately 40% of human genes the first exon is entirely non-coding rather than partly coding [27]. However, our extra 5' sequence is encoded on three exons and the fourth exon contains a translation start codon, suggesting that most or all of these exons contribute coding sequence and the long form translation start codon has yet to be determined.

The mouse DP9 gene is at bases 54,511,520 to 54,543,678 on chromosome 17 (UCSC Genome Browser,

Mouse Feb. 2003 Freeze) and the rat gene at base 888,836 to 913,482 on chromosome 9 (*Rattus norvegicus*.RGSC2.-contig.fa; www.ensembl.org). Examination of mouse full-length cDNA clone AK050021 indicated that human and rodent DP9 sequences diverge near the N-terminus due to rearrangement of the first three exons. In the rat genomic draft, neither a full-length nor a 5' EST of rat cDNA has been isolated in which the translation start codon has been identified. The amino acid sequences of these three proteins converge at Thr1 (rat), Thr17 (mouse) and Thr126 (human). This observation suggests that the rodent and human DP9 genes have diverged at the 5' end to give rise to differences in the N-terminus of each protein.

The potential N-terminal translation start codon located downstream in exon four was tested for its ability to express recombinant protein using reverse transcriptase-PCR amplification from CEM cell line RNA with primers DP9-*Xba*I-Forward and DP9-*Xba*I-Reverse-Fusion generating a 2589-bp DP9 cDNA encoding a 863-amino-acid protein. This cDNA clone of DP9 was subsequently used for enzymology and recombinant protein expression studies.

DP9 is reportedly inactive [28]. However, DP9 contains the catalytic triad Ser-Asp-His and the residues that surround the catalytic serine are Gly-Trp-Ser-Tyr-Gly-Gly in DP9, DP8, DPIV and FAP, suggesting that DP9 has a peptidase activity. Moreover, the DP9 protein sequence contains the two glutamic acid residues that are at position 205 and 206 of DPIV (Fig. 1) and are essential for its dipeptidyl peptidase activity [29]. Interestingly, DP9 contains the Arg-Gly-Asp motif, which is a known integrin binding sequence. Kyte-Doolittle hydrophobicity analysis of the amino acid sequence revealed that DP9, unlike DPIV, FAP, DPL1 and DPL2, contains no potential trans-membrane domain. The DP9 protein contains two potential N-linked glycosylation sites, at residues 313 and 761, so DP9 in contrast to DP8 may contain some glycosylation (Fig. 1). The most significant homology was observed between human DP9 and DP8 (79% amino acid similarity, 61% amino acid identity). A high degree of homology was also observed to both human DPIV (47% amino acid similarity, 26% amino acid identity) and human FAP (46% amino acid similarity, 21% amino acid identity). Human DP9 has 93% and 94% amino acid similarity with mouse and rat DP9, respectively.

In the DPIV family, the consensus sequence around the catalytic serine is [WYF]- Ψ -D-x₂-[RKH]-[Ψ M]-x- Ψ -x-G-W-S-Y-G-G-[YF]-[Ψ M]-[ST]-x₃-[Ψ M], where Ψ is any of the hydrophobic residues Leu, Ile or Val. In the DPL non-enzymes, Asp or Gly replaces the catalytic serine and Lys replaces the preceding Trp. In addition to aligning the catalytic triad, a DPIV gene family alignment (not shown) retained alignment of the DPIV family-defining motif around the pair of glutamates that are essential for peptidase activity and are in the β -propeller domain. We propose that the consensus sequence of this motif is G-

Ψ -x₂-[WFY]- Ψ -[Ψ Y]-[EQ]-E-E-[Ψ FM]-x_{6/7}-W-W-[SC]-P. We have shown that Glu²⁵⁹ of DP8 is essential for enzyme activity [20], so it is very likely the homolog of Glu²⁰⁵ in DPIV. Interestingly, DP9 and DP8 differ from DPIV and FAP at Arg¹²⁵ of DPIV and in having Gln aligned with Glu²⁰⁴ of DPIV (Fig. 1). Glu²⁰⁵, Glu²⁰⁶ and Arg¹²⁵ are the propeller-derived residues that contact substrate in DPIV [30,31]. Moreover, the alignment (Fig. 1) indicates that the N-terminal half (subdomain 1; [30,32]) of the β -propeller domains of DP8 and DP9 differ significantly from that of DPIV. The greatest structural differences between DPIV and prolyl oligopeptidase (PO) are close to the N-terminus [33]. Similarly, the sequence differences between DP9 and DPIV near the N-terminus suggest that the secondary structures of these two enzymes differ significantly in this region.

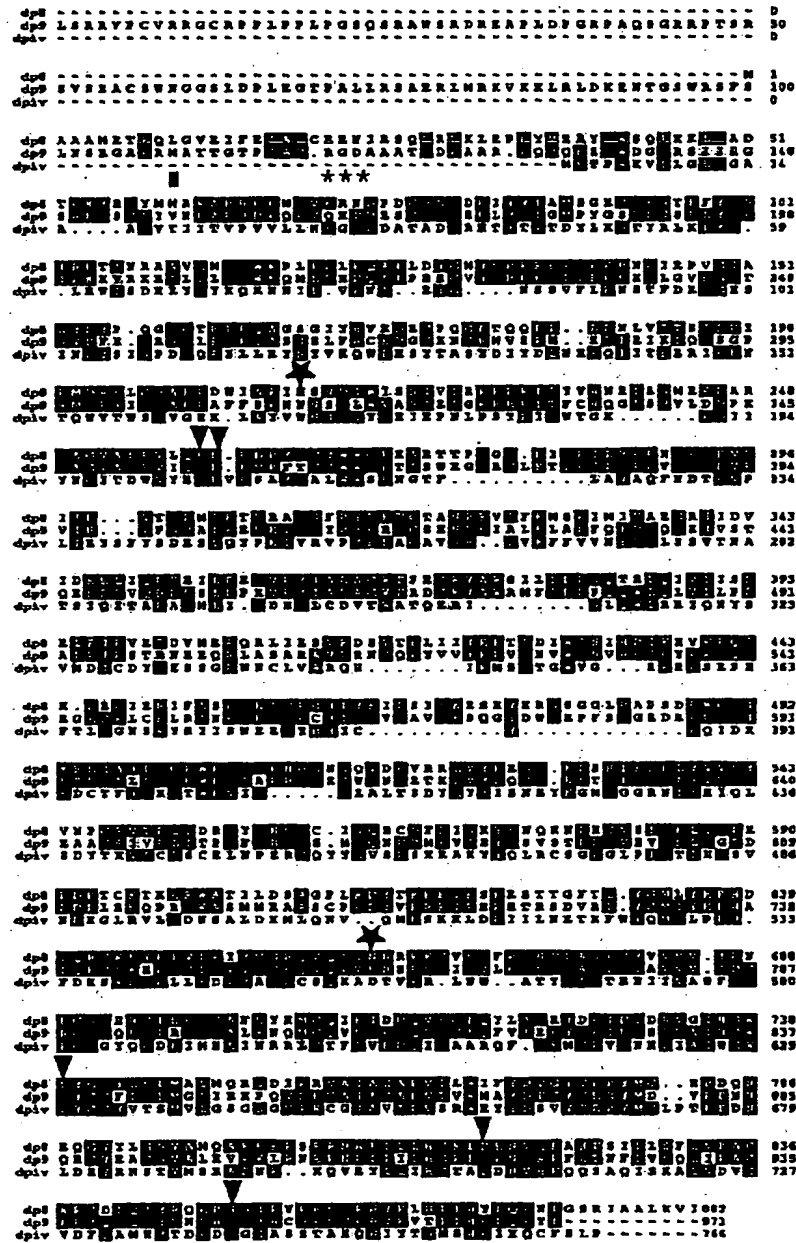
2.2. DP9 expression in human and rat tissues

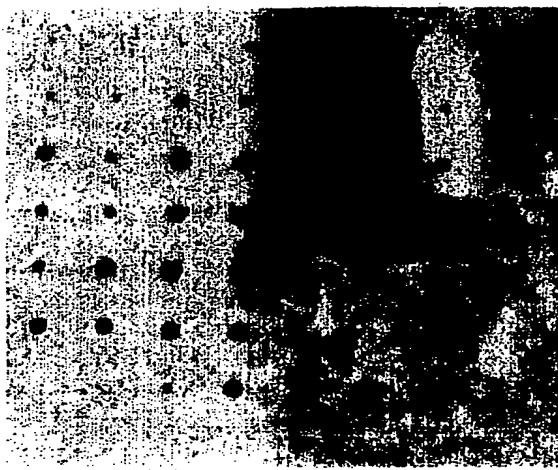
The Master RNA Blot, which used the 3' DP9 PCR product as the probe, demonstrated ubiquitous expression of DP9 in all human adult and foetal tissues (Fig. 2), showing hybridisation patterns that were similar to those obtained using DP8 and DPIV probes (data not shown). There were no signals over any of the negative controls on this blot.

The DP9 Northern blot analysis used two probes: a 1.5-kb PCR product probe from the 3' end of the cDNA and a 306-bp PCR product probe from the 5' end of the long cDNA. Although both probes indicated the presence of transcripts in all tissues examined, the pattern of expression varied (Fig. 3A and B). Using the 3' DP9 probe, a major mRNA transcript of 4.4 kb and a minor mRNA transcript of about 5 kb were detected in most tissues examined. The most abundant signals were in liver, heart, spleen, peripheral blood leukocytes and skeletal muscle. The least expression was observed in the thymus. A smaller transcript approximately 3 kb in size was detected only in liver (Fig. 3A). In contrast, the 5' DP9 probe hybridised only with a 5.0-kb mRNA band on all tissues examined (Fig. 3B). Thus, the weak 5.0-kb mRNA band observed using the 3' probe represented the mRNA transcript for the long DP9 cDNA form. This long DP9 form was most abundant in liver and skeletal muscle.

In silico studies found that most of the 255 human DP9 ESTs (UniGene Cluster Hs.237617) were derived from diseased or tumour tissue (not shown). Interestingly, many ESTs containing sequence specific for the DP9 long form were derived from tumour tissue (Table 2).

To characterise DP9 expression in rodents, a Rat Multiple Tissue Northern blot was hybridised with the human 3' DP9 probe. A 4.0-kb mRNA transcript was detected in all rat tissues, with the most abundant expression in liver, heart and brain (Fig. 3C). A 3.5-kb mRNA transcript was observed in testes and two mRNA transcripts, at 5 to 5.5 kb, were observed in all the tissues tested.





	1	2	3	4	5	6	7	8
A	whole brain	amygdala	caudate nucleus	cerebellum	cerebral cortex	frontal lobe	hippocampus	medulla oblongata
B	occipital lobe	putamen	substantia nigra	temporal lobe	thalamus	sub-thalamic nucleus	spinal cord	
C	heart	aorta	skeletal muscle	colon	bladder	uterus	prostate	stomach
D	testis	ovary	pancreas	pituitary gland	adrenal gland	thyroid gland	salivary gland	mammary gland
E	kidney	liver	small intestine	spleen	thymus	peripheral leukocytes	lymph node	bone marrow
F	appendix	lung	trachea	placenta				
G	fetal brain	fetal heart	fetal kidney	fetal liver	fetal spleen	fetal thymus	fetal lung	
H	yeast tRNA 100 ng	yeast tRNA 100 ng	E. coli tRNA 100 ng	E. coli DNA 100 ng	Poly (A) 100 ng	human Cc1DNA 100 ng	human DNA 100 ng	human DNA 500 ng

Fig. 2. DP9 mRNA expression in human tissues. The Human RNA Master Blot™ (Clontech) containing poly(A)⁺ RNAs from 50 tissues was hybridised with the ³²P labelled 3' DP9 probe. The diagram on the right shows the positions of samples and controls.

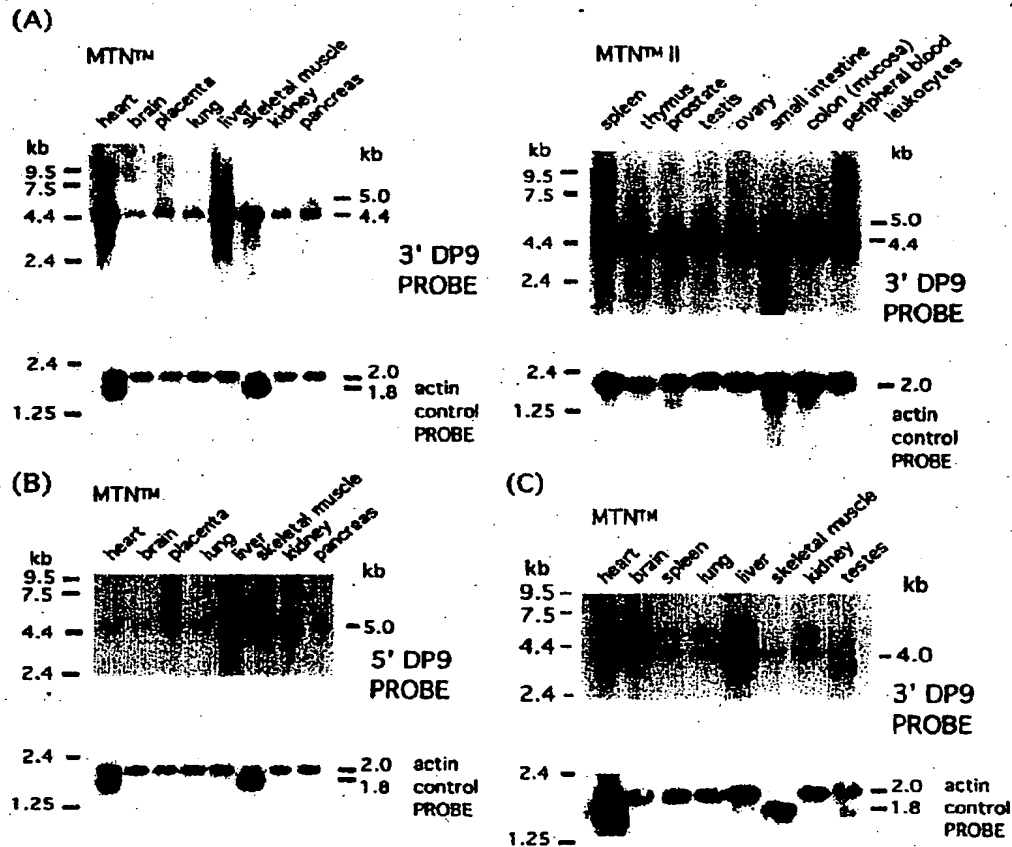


Fig. 3. DP9 Northern blot analysis. Human (A, B) and rat (C) multiple tissue Northern (MTN) blots (Clontech) containing 2 µg per lane poly(A)-rich RNA were hybridised with ³²P-labelled DP9 probes at 68 °C (A, B) or 60 °C (C), then washed at high stringency. These blots were hybridised with probes derived from 3' (A, C) or 5' (B) regions of human DP9.

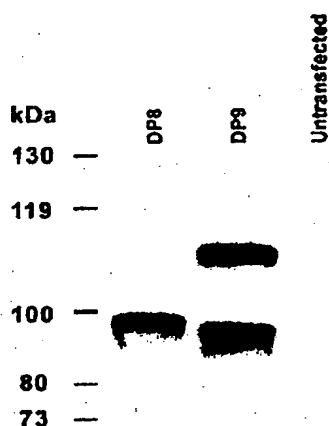


Fig. 4. Recombinant DP9 protein. Soluble aqueous extracts of 1×10^6 transiently transfected 293T cells per lane were run on 8% SDS-PAGE and probed with an anti-V5 mAb in immunoblots. Non-boiled V5-tagged DP8 protein ran at the expected gel mobility of about 100 kDa [19]. Non-boiled, V5-tagged DP9 protein produced bands at about 95 and 110 kDa. Representative data from four experiments.

(Fig. 4). DP8/V5/His was seen as a characteristic monomer at about 100 kDa. Both DP9/V5/His and DP8/V5/His were detected in the cytoplasm, including Golgi, but not on the cell surface by flow cytometry (Fig. 5) and immunofluorescence (Fig. 6).

DPIV has a soluble extracellular form, so we sought evidence of DPs in cell culture supernatants. Up to eightfold more peptidase activity was detected in cell culture supernatants from DPIV-transfected cells than vector-transfected cells collected 7 days post transfection (Table 3). In contrast, DP9 or DP8 transfection did not increase the peptidase activity of cell culture supernatant. All DP9 protein data reported here derived from preparations in which more than 30% of the cells expressed recombinant protein.

2.4. DP9 is a dipeptidyl peptidase

Permeabilised DP9-transfected 293T cells were examined for proline-specific peptidase activity. DPIV and DP8 expressed in 293T cells were used as positive controls. The negative controls, untransfected and vector-only-transfected 293T cells, exhibited very little endogenous activity and all

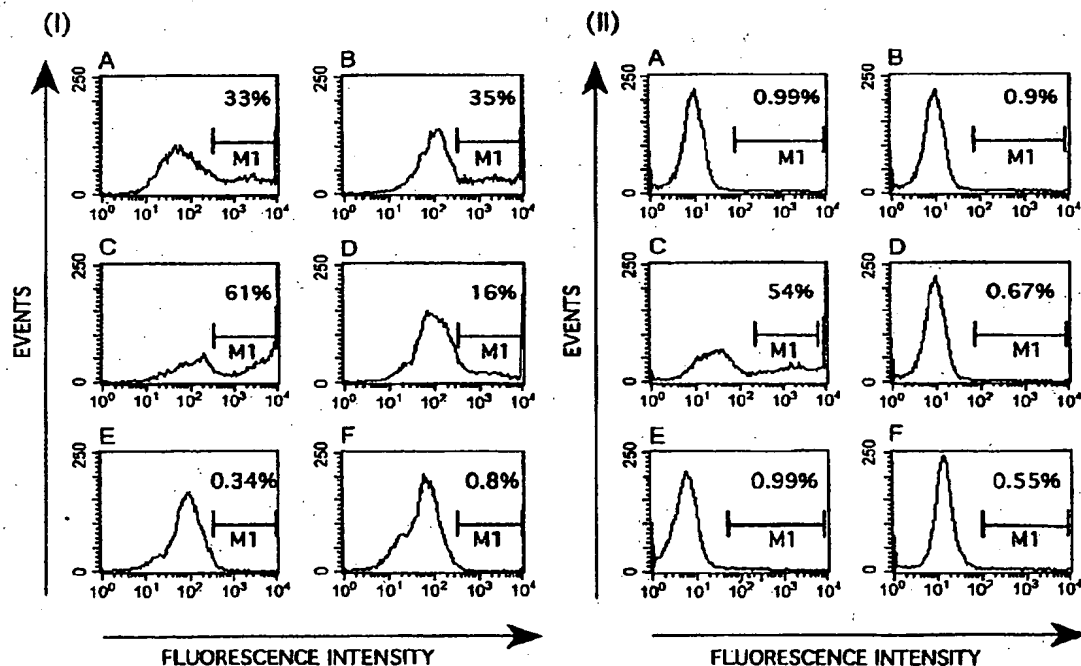


Fig. 5. DP9 is not cell surface expressed. Recombinant protein expression was detected by staining transfected 293T cells with a mAb to the V5 epitope tag. Cell permeabilisation (panel I) permits antibody entry into cells to detect internal expression of recombinant protein, whereas antibody staining of intact cells (panel II) detects only cell surface expression. Cells transfected with either of two replicate cDNA clones of DP9 (A and B) were immunostained only when the cells were permeabilised (IA; IB), thus demonstrating the cytoplasmic expression of DP9. In contrast, both intact (IIC) and permeabilised (IC) cells transfected with V5-tagged DPIV were immunopositive, demonstrating cell surface expression. DP8 expression was detected only in permeabilised cells (ID). Negative controls included untransfected (E) and vector-transfected (F) cells. The percentage of cells immunopositive (gate M1) is shown in each panel. Representative data from three experiments.

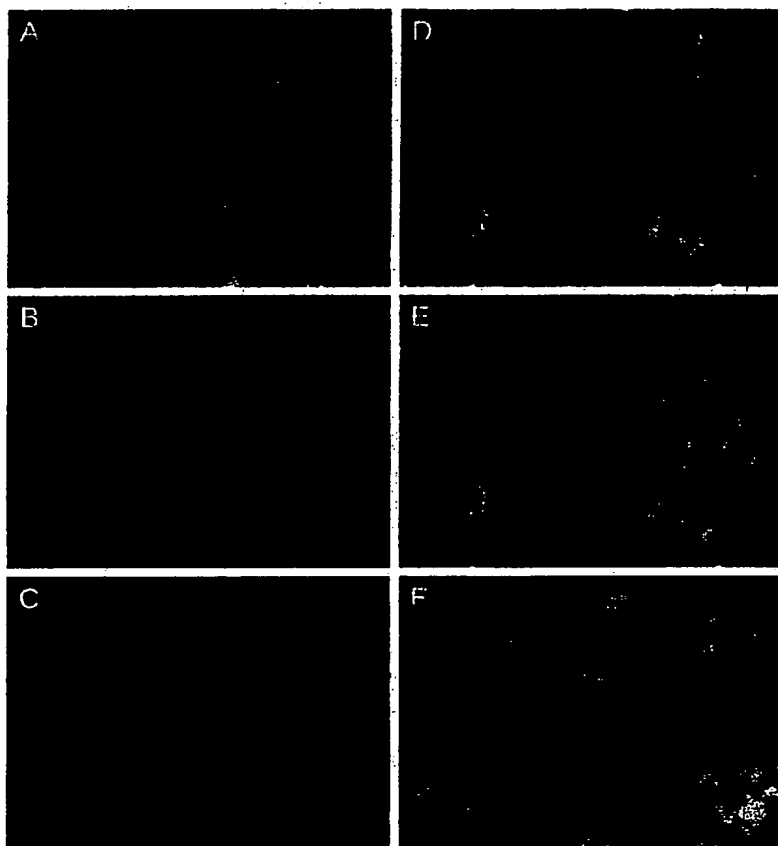


Fig. 6. DP9 expression is cytoplasmic. Fluorescence microscopy of permeabilised 293T cells. Transfected cells expressing V5 epitope tagged DP9 (A—tricolour, B—anti-V5 and Texas Red, C—wheat germ agglutinin-FITC), DPIP (D), DP8 (E) or untransfected cells (F) were stained with anti-V5 mAb followed by Texas Red conjugated goat anti-mouse Ig. Golgi were stained green using wheat germ agglutinin-FITC. The nuclei were stained blue with DAPI. Original magnification $\times 400$.

assay data were corrected for this endogenous activity. DP9-transfected 293T cells specifically hydrolysed Ala-Pro-AFC (Table 4) and Gly-Pro-pNA (not shown). Further negative controls included several cDNA clones of DP8 that contained activity-ablating point mutations [20], indi-

cating that the peptidase activity was a property of DP9 rather than of DP-transfected cells.

3. Discussion

We previously noted that a gene at 19p13.3 has significant homology with DP8 and named this gene DP9 [19]. We now report in detail the isolation of a 2589-bp and a longer 3006-bp DP9 sequence and their characterization.

Table 3
DPIP, but not DP8 or DP9, was detected in cell culture supernatant of transfected cells

	cDNA transfected			
	DPIP	DP8	DP9	None
293T cells. Substrate H-Ala-Pro-pNA (Δ absorbance/min $\times 1000$).	$8.4 \pm 1.4^*$	1.3 ± 0.4	ND	1.4 ± 0.5
COS-7 cells. Substrate H-Ala-Pro-AFC (Δ fluorescence/min).	869.9 ± 15.9	ND	317 ± 13.1	376.4 ± 33.9

* Mean and standard deviation of four replicates. ND = not done.

Table 4
Michaelis–Menten kinetics of DP9, DP8 and DPIP with substrate H-Ala-Pro-AFC

Enzyme	K_m (mM)	V_{max} (Δ fluorescence/min)	Δ Fluorescence/min/ 10^6 cells
DP9	0.18 ± 0.07	268.5 ± 23.1	1342.5 ± 115.5
DP8	0.18 ± 0.02	237.5 ± 7.2	1187.5 ± 36
DPIP	0.638 ± 0.3	462.6 ± 62.5	2313 ± 312.5

The longer sequence corresponds to a distinctly larger transcript that was most readily detected in human muscle, spleen and peripheral blood leukocytes. The two distinct transcript sizes were ubiquitous and seen in both human and rat tissues. DP9 exhibited peptidase activity against Ala-Pro and Gly-Pro derived dipeptide substrates. We found that DP9 is a monomeric, soluble, cytoplasmic protein, characteristics it shares with DP8 and PO but not with DPIV, FAP, DPL1 or DPL2.

By homology with DPIV, DP9 is a member of the DPIV gene family, a member of the DPIV subfamily S9b of PO family S9 in enzyme clan SC. The residues in DP8 that form the charge-relay system are Ser⁷³⁹, Asp⁸¹⁷ and His⁸⁴⁹ [20] and the equivalent residues in DP9 are Ser⁸³⁸, Asp⁹¹⁶ and His⁹⁴⁸ (Fig. 1). Furthermore, the DP9 enzyme activity was very similar to DPIV and DP8. Our data is supported by the very recent report that the 863-amino-acid DP9 protein is enzymatically active [18] rather than inactive as reported previously [28].

Discriminating between the four enzymes of the DPIV family is difficult because their monomeric sizes are all between 95 and 110 kDa and they all hydrolyse H-Ala-Pro derived substrates. FAP and DPIV are integral membrane glycoproteins and require dimerization for catalytic activity [13,20,34–36]. In contrast, DP9 and DP8, like PO, are cytosolic proteins that are catalytically active as monomers and cleave the post-proline bond, in Pro-Xaa [18,19,37]. However, the substrate specificity of PO is distinct from DP9. PO is an endopeptidase that does not cleave if a free α -amine lies N-terminal to the proline (i.e. it does not cleave H-Ala-Pro-AFC). Although the DPIV and PO tertiary structures both contain an α/β -hydrolase domain they differ in the β -propeller domain. Primarily, PO has a seven-blade β -propeller and DPIV has an eight-blade β -propeller [30,33]. The significant sequence identities between DP9, DP8, FAP and DPIV suggest that the tertiary structures of DP9, DP8, FAP and DPIV are similar. However, DP8 and the short form of DP9 contain more than 100 amino acids more than DPIV, so DP9 and DP8 could have an additional element of tertiary structure at the N-terminus or a larger β -propeller domain with additional protrusions.

The 863-amino-acid DP9 protein is predicted to have a polypeptide backbone of 98,263 Da. Monomers of 95 and 110 kDa were detected in immunoblots of transfected cells (Fig. 4). The 110-kDa band perhaps represents a glycosylated form and the 95-kDa band a breakdown product, analogous to the 100 and 80-kDa bands of DP8 [19], which has 882 amino acids. Chimeras of DPIV with the α/β -hydrolase domains of DP9 and DP8 indicate that the α/β -hydrolase domain of DP9 is glycosylated [20]. Moreover, the size difference between DP9 and DP8 (Fig. 4) is greater than the size difference between the DPIV–DP9 chimera and the DPIV–DP8 chimera [20], suggesting that the β -propeller domain of DP9 is also glycosylated.

The biological significance of the larger splice variant of DP9 that we discovered is unknown. The additional se-

quence is at the 5' end, so both forms contain the residues required for peptidase activity. Alternate splice forms of DP8 and of FAP mRNA have also been observed [19,38]. The additional 5' cDNA sequence in the DP9 long form lacks homology with any other protein. However, some other members of this gene family are larger than DP9. The *D. melanogaster* ortholog closest to DP8 and DP9 (Q9VC19) is 1102 amino acids long but shares no homology with this family in the N-terminal 200 amino acids. We propose that the major transcripts for human DP9 mRNA lie within the 4.4-kb band and the 5-kb transcript may contain additional 5' translated or untranslated sequence. Our observation that many ESTs that contain this additional DP9 5' sequence derive from lymphocytic cell lines and tumours indicates that the long DP9 form is expressed in tumours. DP9 is similar to DPIV and DP8 in having a ubiquitous mRNA expression pattern. The similarities between DP9, DP8 and DPIV suggest that DP9 and DP8 may, like DPIV, have roles in diverse biological processes.

Interestingly, the serine recognition site, GWSYGG, is found in a single exon in human DP9 and DP8, the *C. elegans* homolog of DP8 and DP9 (GenBank O44987) and the mouse and *C. elegans* homologs of PO. This differs from the arrangement in the DPL1, DPL2 and *C. elegans* and human DP4 genes and human FAP and mouse Fap genes where the serine recognition site spans two exons. Thus, the gene arrangement in PO, DP9 and DP8 is representative of the ancestral PO (S9) family gene and the arrangement in DPL1, DP4 and FAP has resulted from divergent evolution from this ancestral gene [1]. While DP4, FAP and DPL2 have been localized to the long arm of chromosome 2, at 2q24.2, 2q24.3 and 2q12.3–14.2, respectively, DP8 has been localized to 15q22.31 and DP9 to 19p13.3. The related genes DPL1 and PO have been localized to 7q36.2–7q36.3 and 6q21, respectively [39].

Disease loci mapped to chromosome 19p13.3 include susceptibility to polycystic ovary syndrome [40] and atherogenic lipoprotein phenotype [41]. Interestingly, many patients with polycystic ovary syndrome develop obesity and insulin resistance and a gene (*Beacon*) that is linked to obesity in the fat sand rat *Psammomys obesus*, lies in a region syntenic to human 19p13.3 [42]. Chromosome 19p13.3 is gene-rich and further studies are needed to establish a link between DP9 and any of these diseases. However, the prominent expression of DP9 in muscle and liver is consistent with a role in lipid metabolism.

DP9 is the fourth enzyme of the S9b family. We have cloned, expressed and characterized this novel human dipeptidyl aminopeptidase and found structural and functional differences as well as similarities to DP8, DPIV and FAP. With many diverse biological roles suggested for DPIV, particularly in the endocrine and immune systems, and the roles of FAP in tumor growth and liver disease, it will be interesting to investigate the roles of this new member of the DPIV gene family in these systems. Further work in understanding this novel protein and the elucidation

of its inhibitor and substrate specificities will help identify the specific functions of individual members of this gene family.

Acknowledgements

We thank Xin M. Wang for assistance with imaging the immunofluorescence, Mina Obradovic for some initial DP8 transfection experiments and Ingrid de Meester for critical comments on the paper.

References

- [1] C.A. Abbott, M.D. Gorrell, The family of CD26/DPIV and related ectopeptidases, in: J. Langner, S. Ansorge (Eds.), *Ectopeptidases: CD13/Aminopeptidase N and CD26/Dipeptidylpeptidase IV in Medicine and Biology*, Vol., Kluwer/Plenum, NY, 2002, pp. 171–195.
- [2] B. Leiting, K.D. Pryor, J.K. Wu, F. Marsilio, R.A. Patel, C.S. Craik, J.A. Ellman, R.T. Cummings, N.A. Thornberry, Catalytic properties and inhibition of proline-specific dipeptidyl peptidases II, IV and VII, *Biochem. J.* 371 (2003) 525–532.
- [3] M.D. Gorrell, V. Gysbers, G.W. McCaughan, CD26: a multifunctional integral membrane and secreted protein of activated lymphocytes, *Scand. J. Immunol.* 54 (2001) 249–264.
- [4] A.-M. Lambeir, C. Durinx, S. Scharpe, I. De Meester, Dipeptidyl peptidase IV from bench to bedside: An update on structural properties, functions and clinical aspects of the enzyme DPP IV, *Crit. Rev. Clin. Lab. Sci.* 40 (2003) 209–294.
- [5] J. Langner, S. Ansorge, *Ectopeptidases: CD13/Aminopeptidase N and CD26/Dipeptidylpeptidase IV in Medicine and Biology*, Kluwer/Plenum, NY, 2002, p. 383.
- [6] H. Kajiyama, F. Kikkawa, T. Suzuki, K. Shibata, K. Ino, S. Mizutani, Prolonged survival and decreased invasive activity attributable to dipeptidyl peptidase IV overexpression in ovarian carcinoma, *Cancer Res.* 62 (2002) 2753–2757.
- [7] S. Conarello, Z. Li, J. Ronan, R. Roy, L. Zhu, G. Jiang, F. Liu, J. Woods, E. Zychband, D. Moller, N. Thornberry, B. Zhang, Mice lacking dipeptidyl peptidase IV are protected against obesity and insulin resistance, *Proc. Natl. Acad. Sci. U. S. A.* 100 (2003) 6825–6830.
- [8] K. Augustyns, P. Van der Veken, K. Senten, A. Haemers, Dipeptidyl peptidase IV inhibitors as new therapeutic agents for the treatment of Type 2 diabetes, *Expert Opin. Ther. Pat.* 13 (2003) 499–510.
- [9] D.J. Drucker, Therapeutic potential of dipeptidyl peptidase IV inhibitors for the treatment of type 2 diabetes, *Expert Opin. Investig. Drugs* 12 (2003) 87–100.
- [10] D.A. Fox, R.E. Hussey, K.A. Fitzgerald, O. Acuto, C. Poole, L. Palley, J.F. Daley, S.F. Schlossman, E.L. Reinherz, Tal, a novel 105 KD human T cell activation antigen defined by a monoclonal antibody, *J. Immunol.* 133 (1984) 1250–1256.
- [11] C. Durinx, A.M. Lambeir, E. Bosmans, J.B. Falmagne, R. Berghmans, A. Haemers, S. Scharpe, I. De Meester, Molecular characterization of dipeptidyl peptidase activity in serum—soluble CD26/dipeptidyl peptidase IV is responsible for the release of X-Pro dipeptides, *Eur. J. Biochem.* 267 (2000) 5608–5613.
- [12] P. Garin-Chesa, L.J. Old, W.J. Rettig, Cell surface glycoprotein of reactive stromal fibroblasts as a potential antibody target in human epithelial cancers, *Proc. Natl. Acad. Sci. U. S. A.* 87 (1990) 7235–7239.
- [13] M.T. Levy, G.W. McCaughan, C.A. Abbott, J.E. Park, A.M. Cunningham, W.J. Rettig, M.D. Gorrell, Fibroblast activation protein: a cell surface dipeptidyl peptidase and gelatinase expressed by stellate cells at the tissue remodelling interface in human cirrhosis, *Hepatology* 29 (1999) 1768–1778.
- [14] K. Wada, N. Yokotani, C. Hunter, K. Doi, R.J. Wenthold, S. Shimaseki, Differential expression of two distinct forms of mRNA encoding members of a dipeptidyl aminopeptidase family, *Proc. Natl. Acad. Sci. U. S. A.* 89 (1992) 197–201.
- [15] L. de Lecea, E. Soriano, J.R. Criado, S.C. Steffensen, S.J. Henriksen, J.G. Sutcliffe, Transcripts encoding a neural membrane CD26 peptidase-like protein are stimulated by synaptic activity, *Brain Res. Mol. Brain Res.* 25 (1994) 286–296.
- [16] M. Allen, A. Heinzmann, E. Noguchi, G. Abecasis, J. Broxholme, C.P. Ponting, S. Bhattacharyya, J. Tinsley, Y. Zhang, R. Holt, E.Y. Jones, N. Lench, A. Carey, H. Jones, N.J. Dickens, C. Dinton, R. Nicholls, C. Baker, L. Xue, E. Townsend, M. Kabesch, S.K. Weiland, D. Carr, E. von Mutius, I.M. Adcock, P.J. Barnes, G.M. Lathrop, M. Edwards, M.F. Moffatt, W.O. Cookson, Positional cloning of a novel gene influencing asthma from chromosome 2q14, *Nat. Genet.* 35 (2003) 258–263.
- [17] T. Chen, K. Ajami, G.W. McCaughan, M.D. Gorrell, C.A. Abbott, Dipeptidyl peptidase IV gene family, *Adv. Exp. Med. Biol.* 524 (2003) 79–86.
- [18] S.Y. Qi, P.J. Riviere, J. Trojnar, J.L. Junien, K.O. Akinsanya, Cloning and characterization of dipeptidyl peptidase 10, a new member of an emerging subgroup of serine proteases, *Biochem. J.* 373 (2003) 179–189.
- [19] C.A. Abbott, D.M.T. Yu, E. Woollatt, G.R. Sutherland, G.W. McCaughan, M.D. Gorrell, Cloning, expression and chromosomal localization of a novel human dipeptidyl peptidase (DPP) IV homolog, DPP8, *Eur. J. Biochem.* 267 (2000) 6140–6150.
- [20] K. Ajami, C.A. Abbott, M. Obradovic, V. Gysbers, T. Kahne, G.W. McCaughan, M.D. Gorrell, Structural requirements for catalysis, expression and dimerisation in the CD26/DPIV gene family, *Biochemistry* 42 (2003) 694–701.
- [21] T. Tanaka, D. Camerini, B. Seed, Y. Torimoto, N.H. Dang, J. Kameoka, H.N. Dahlberg, S.F. Schlossman, C. Morimoto, Cloning and functional expression of the T cell activation antigen CD26, *J. Immunol.* 149 (1992) 481–486.
- [22] S.F. Altschul, W. Gish, W. Miller, E.W. Myers, D.J. Lipman, Basic local alignment search tool, *J. Mol. Biol.* 215 (1990) 403–410.
- [23] W.J. Kent, BLAT—the BLAST-like alignment tool, *Genome Res.* 12 (2002) 656–664.
- [24] S. Mizushima, S. Nagata, pEF-BOS, a powerful mammalian expression vector, *Nucleic Acids Res.* 18 (1990) 5322.
- [25] C.A. Abbott, G.W. McCaughan, M.T. Levy, W.B. Church, M.D. Gorrell, Binding to human dipeptidyl peptidase IV by adenosine deaminase and antibodies that inhibit ligand binding involves overlapping, discontinuous sites on a predicted beta propeller domain, *Eur. J. Biochem.* 266 (1999) 798–810.
- [26] A.J. Barratt, N.D. Rawlings, E.A. O'Brien, The MEROPS database as a protease information system, *J. Struct. Biol.* 134 (2001) 95–102.
- [27] R.V. Davuluri, I. Grosse, M.Q. Zhang, Computational identification of promoters and first exons in the human genome, *Nat. Genet.* 29 (2001) 412–417.
- [28] C. Olsen, N. Wagtmann, Identification and characterization of human Dpp9, a novel homologue of dipeptidyl peptidase IV, *Gene* 299 (2002) 185–193.
- [29] C.A. Abbott, G.W. McCaughan, M.D. Gorrell, Two highly conserved glutamic acid residues in the predicted beta propeller domain of dipeptidyl peptidase IV are required for its enzyme activity, *FEBS Lett.* 458 (1999) 278–284.
- [30] H.B. Rasmussen, S. Branner, F.C. Wiberg, N. Wagtmann, Crystal structure of human DPP-IV/CD26 in complex with a substrate analogue, *Nat. Struct. Biol.* 10 (2003) 19–25.
- [31] R. Thoma, B. Löffler, M. Stihle, W. Huber, A. Ruf, M. Hennig, Structural basis of proline-specific exopeptidase activity as observed in human dipeptidyl peptidase-IV, *Structure* 11 (2003) 947–959.
- [32] M.D. Gorrell, First bite, *Nat. Struct. Biol.* 10 (2003) 3–5.
- [33] H. Hiramatsu, K. Kyono, Y. Higashiyama, C. Fukushima, H. Shima, S. Sugiyama, K. Inaka, A. Yamamoto, R. Shimizu, The structure and

- function of human dipeptidyl peptidase IV, possessing a unique eight-bladed beta-propeller fold, *Biochem. Biophys. Res. Commun.* 302 (2003) 849–854.
- [34] G. Puschel, R. Mentlein, E. Heymann, Isolation and characterization of dipeptidyl peptidase IV from human placenta, *Eur. J. Biochem.* 126 (1982) 359–365.
- [35] I. De Meester, G. Vanhoof, D. Hendriks, H.U. Demuth, A. Yaron, S. Scharpé, Characterization of dipeptidyl peptidase IV (CD26) from human lymphocytes, *Clin. Chim. Acta* 210 (1992) 23–34.
- [36] M.L. Pinciro-Sanchez, L.A. Goldstein, J. Dodi, L. Howard, Y. Yeh, W.T. Chen, Identification of the 170-kDa melanoma membrane-bound gelatinase (seprase) as a serine integral membrane protease, *J. Biol. Chem.* 272 (1997) 7595–7601.
- [37] F. Goossens, I. De Meester, G. Vanhoof, D. Hendriks, G. Vriend, S. Scharpé, The purification, characterization and analysis of primary and secondary-structure of prolyl oligopeptidase from human lymphocytes. Evidence that the enzyme belongs to the alpha/beta hydrolase fold family, *Eur. J. Biochem.* 233 (1995) 432–441.
- [38] J. Niedermeyer, M.J. Scanlan, P. Garin-Chesa, C. Daiber, H.H. Fiebig, L.J. Old, W.J. Rettig, A. Schnapp, Mouse fibroblast activation protein: molecular cloning, alternative splicing and expression in the reactive stroma of epithelial cancers, *Int. J. Cancer* 71 (1997) 383–389.
- [39] J.D. McPherson, M. Marra, L. Hillier, R.H. Waterston, A. Chinwalla, J. Wallis, M. Sekhon, K. Wylic, F.R. Mardis, R.K. Wilson, R. Fulton, T.A. Kucaba, C. Wagner-McPherson, W.B. Barbazuk, S.G. Gregory, S.J. Humphray, L. French, R.S. Evans, G. Bethel, A. Whittaker, J.L. Holden, O.T. McCann, A. Dunham, C. Soderlund, C.F. Scott, T.I.H.G.M. Consortium, et al., A physical map of the human genome, (<http://genome.ucsc.edu/>) *Nature* 409 (2001) 934–941.
- [40] S. Tucci, W. Futterweit, E.S. Concepcion, D.A. Greenberg, R. Villanueva, T.F. Davies, Y. Tomer, Evidence for association of polycystic ovary syndrome in caucasian women with a marker at the insulin receptor gene locus, *J. Clin. Endocrinol. Metab.* 86 (2001) 446–449.
- [41] M.A. Wride, F.C. Mansergh, J.M. Somani, R.J. Winkfein, D.E. Rancourt, Characterization and in silico mapping of a novel murine zinc finger transcription factor, *Gene* 289 (2002) 49–59.
- [42] L. Kantham, L. Kerr-Bayles, N. Godde, M. Quick, R. Webb, T. Sunderland, J. Bond, K. Walder, G. Augert, G. Collier, Bcocon interacts with cdc2/cdc28-like kinases, *Biochem. Biophys. Res. Commun.* 304 (2003) 125–129.